Scour around Cross-Threaded Piers in Regular Waves

By:

Shadana Gupta d/o Baldev Raj

16773

Dissertation submitted in partial fulfilment of

the requirement for the

Bachelor of Engineering (Hons)

(Civil Engineering)

JANUARY 2015

Universiti Teknologi PETRONAS

Bandar Seri Iskandar

31750 Tronoh,

Perak Darul Ridzuan

CERTIFICATION OF APPROVAL

Scour around Cross-Threaded Piers in Regular Waves

by

Shadana Gupta d/o Baldev Raj

16773

A project dissertation submitted to the

Civil Engineering Programme

Universiti Teknologi PETRONAS

in partial fulfilment of the requirement for the

BACHELOR OF ENGINEERING (Hons)

(CIVIL ENGINEERING)

Approved by,

_____

(Dr. Teh Hee Min)

UNIVERSITI TEKNOLOGI PETRONAS

TRONOH, PERAK

January 2015

CERTIFICATION OF ORIGINALITY

This is to certify that I am responsible for the work submitted in this project, that the original work is my own except as specified in the references and acknowledgements, and that the original work contained herein have not been undertaken or done by unspecified sources or persons.

_____

SHADANA GUPTA D/O BALDEV RAJ

ABSTRACT

This paper conducted the experiment on the formation scour around cross-threaded piers subjected to regular waves. The factor formations of scour had been identified by extensive research of previous paper that related to the project. From the gap of previous research, the project constructed physical model of the protected and unprotected pile. This study used cross-threaded pile as a flow-altering countermeasure mechanism to obtain results on average of scour reduction compared unprotected pier with variation of cable diameter and thread angle. The flow pattern around the pile was observed and the effect of wave period on the formation of scour was analysed. However, with the time constraint and the availability of the instrument, only a few test series and wave condition studied in this paper. As the results the single cross-threaded piers and double cross-threaded piers were able to reduce scour in average of 42% and 28%. That shows the cable-pier diameter ratio and thread angle influent the performance of models in scour reduction. The small number of cross-threaded pier with smaller cable-pier diameter ratio and small thread angle will give the best performance in reducing potential formation of scour depth. As recommendation for future research, other types of flow-altering countermeasure mechanism and its efficiency in wave condition can be studied for more details and strong hypothesis.

ACKNOWLEDGEMENT

The author would like to express her gratitude to the supervisor, Dr. Teh Hee Min; lecturer of Civil Engineering Department, Universiti Teknologi PETRONAS who has guided the author through this project dedicatedly. Dr. Teh Hee Min is always generous in sharing his thoughts and ideas and has never hesitated to give guidance and support throughout this whole project, for which I am greatly thankful for.

To my friends; Yim Kit Yen and Mohamad Zulkarnain Bin Mohamed Mokhtar, thank you for all the helps during experimental works. Your contributions are highly appreciated.

To my family members, thank you for your full support and encouragement that has enabled me to complete this whole project successfully.

Lastly, my appreciation also goes out to the technicians and whoever else that has been involved in some ways or other in helping me to carry out this project successfully.

Thank you,

SHADANA GUPTA D/O BALDEV RAJ

Civil Engineering

CONTENTS

SYMBOLS

b	=	cable diameter;
D	=	pier diameter;
θ	=	thread angle;
d_{50}	=	median diameter of bed sand;
y	=	scour depth of protected pier;
s_0	=	scour depth of unprotected pier;
a	=	pier width;
h	=	water depth;
g	=	acceleration of gravity (9.81 m/s^2);
b/D	=	cable diameter to pier diameter ratio;
T	=	wave period;
d	=	water depth;
L	=	wave length;
H	=	wave height

LIST OF FIGURES

LIST OF TABLES

CHAPTER 1
INTRODUCTION

1.1 General

A typical marine structure is made of two main structural components which is the superstructure and the substructure. The substructure component includes piers, columns, footing, and piles, which are used for transferring the loads to the foundation bed. Piles connect the substructure of the bridge to the foundation. The presence of water that flows through the piles and around the columns can result in an erodible foundation bed, hence changing the flow pattern around the substructure. These changes in flow may contribute strength in transporting of sediment, further leading to scouring. Water that flows above sediment beds, either in rivers or in the sea, may cause erosion. Sediment transport occurs due to the existence of an interface between the flow and the moving boundary.

Wave scouring is a major concern for any structure that been designed and used in marine-based environment Wave scouring results in structural failures, when exposed to excessive wave flows and unpredictability in ocean conditions.

There are two types of scours, namely local scour and global scour. Local scour occurs due to the existence of an obstacle to the flow, such as a bridge pier or abutment. Whereas global erosion occurs naturally, without the existence of an obstacle. Scour may occur under two different flow conditions which is the clean-water scour and live-bed scour. Clear-water scour happens when there is no transport of bed material upstream from the structure. Live-bed scour occurs when there is bed material transport upstream from the structure, and is cyclic in nature.

The basic mechanism causing local scour is the formation of vortices at the base which is known as horseshoe vortex. Factors that influence the magnitude of maximum piers scour depth are the flow approach velocity, depth of flow, the pier transversal dimension, the water depth, the pier length if it is not aligned with the

main stream direction, the angle of attack of the approach flow to the pier, the pier's shape, the size and gradation of bed material.

The piers protection against local scour is a point of great importance in the safety of bridges, since excessive scour may decrease the quality of its structural function, or even lead to its collapse. Countermeasures against pier scour can be classified into two categories which is the flow-altering countermeasures and bed-armouring countermeasures. The operating principle of the flow altering countermeasures is to decrease the intensity of the down flow and horseshoe vortex, which are the main cause of local scour. Moreover, the bed-armouring countermeasures consist in the creation of a physical barrier (as in the case of riprap, gabions or cable-tied blocks) against possible local scour.

1.2 Background of study

Scour a natural phenomenon that involves the erosion, transport and deposition of sediment of stream bed in variety of situations. This relates to erosive action of water that the flows carries and excavate away materials or sediment from the banks of bed of the stream. While local scour is the results of erosion that occurs over a region of limited extend due to local flow conditions caused by the structure that obstruct the flow pattern as seen in ***Figure 1-1***. The stability of structure decreases as the formation/depth of scour increases due to losing its bearing capacity at foundation.

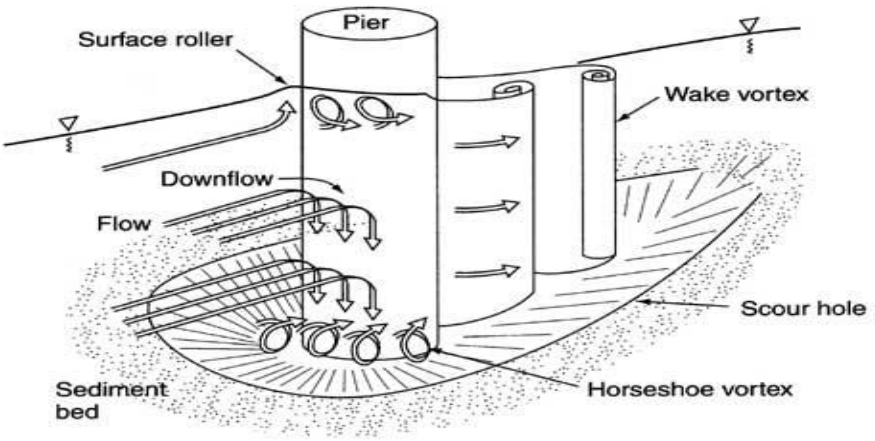

Figure 1-1*: Main Features of Flow around a Bridge Pier (Retrieve From: Hamill, 1998)*

In case of cylindrical piles a down flow is observed at the upstream nose of the pier, and a horseshoe vortex develops due to the pileup of water on the upstream surface of the obstruction and subsequent acceleration of the flow around the nose of the pier. The simultaneous action of the downward flow and the separated flow, which occurs as a result of the change of pressure field. This generates a horseshoe vortex, considered primarily responsible for the formation of local scour process.

The scour hole increases in both depth and extending upstream, while the horseshoe vortex continues to dig the bed. Sediments are transported downstream, and eventually settle in regions of lower turbulence. As the depth of scour increases the transport rate from the base of the pier diminishes. For clear-water scour, the scour process ceases when the shear stress caused by the horseshoe vortex equals the critical shear stress of the sediment particles at the bottom of the scour hole.

Jetties, seawall or bridge, pile groups obstructs wave and current pattern, resulting in formation of scour due to expose of foundation. The reliability of marine structure is directly related to the scour depth formed at their toes due to waves and current. Therefore, it is important to determine the maximum possible scour depth of the designed marine structure.

1.3 Problem Statement

The study of scour under the influence of waves is well established. However, scour at the lee of the pier still exists due to the exposed pier to excessive wave energy. This flow has not been sufficiently dissipated by the friction of toe protection. Besides the structure interaction which resulting the formation of wake vortices at the lee of pier are undermining the soil material. Thus, reduction of local scour rate might be achievable through altering the flow direction when passing around the pier. Various empirical equations have been reported for calculation of the scour properties for example scour depth, scour width, Keulegan–Carpenter number and etc. Many ingenious designs of countermeasures against scour have been proposed, developed and tested in the last decade. One of the measures is to correct the flow direction by the cross-threaded pier.

Dey, Sumer and Fredsøe (2006) investigated scour due to threaded piers wave conditions with few type of thread angle and size while Tafarojnoruz, Gaudio, and Calomino (2012) only investigated in currrent only condition. Nevertheless, scour due to cross-threaded piers subjected to regular wave only condition has not been explored. This research is motivated to investigate effieciney of the cross-threaded piers of different properties such as thread angle and diameter of cable in regular wave via physical modeling.

1.4 Objective

This research aims at investigating the effect of the cross-threaded pier on scour under regular waves via physical modelling. To achieve the goal, the following objectives are skeletoned :

1. To determine the scour depth of a unprotected pier.
2. To determine the scour depth of cross-threaded piers.
3. To determine the efficiency of the cross-threaded piers in reducing scour depth.

1.5 Scope of work

In order to achieve the objectives, the study has been divided into five major elements:

1. Literature Review

   Extensive studies on previous research related to scour has to be carried out. The research problem and gap have to be identified related to scour and addressed accordingly through desktop study.

2. Model Fabrication

   A number of test models are to be constructed for the study of their efficiency in reducing scour in wave action. The models were fabricated in the lab with proposed material and dimension. Two type of countermeasure were introduce with mix and match method for different dimension.

3. Laboratory Set Up

   Setting up the equipment required for the experiment to ensure they are in good working condition. Apparatus and equipment used for experiments will be checked for the accuracy of the experiment results obtained. The models will be tested in open channel flume. The flume set-up based on previous research as to make the result is comparable such as sediment size and models dimension.

4. Experiment

   A physical model will be constructed and an experimental study will conducted in order to fill the gap between the previous researches and for improvement purposes. There are a number models of series of different type of models with different properties will be tested.

5. Analysis of Results

   The result from this experimental will be interpreted for better understanding on the subject of the study.

CHAPTER 2
LITERATURE REVIEW AND THEORY

2.1 Introduction

One of the causes associated with the collapse of marine structure is the phenomenon of scour around piers. Understanding of the maximum scour depth that potentially exists around the piers would help the design of piers and toe protection. The depth of scour may vary depends on type of the flow, type of the structures and condition of sediment. This part of chapter will be focusing on the wave scouring at marine structure, types of failure due to scouring, evaluation criteria for scour and some type of countermeasures for scour reduction.

2.2 Wave Scouring at Marine Structure

Scour is defined as the carried away of granular material near marine structures, which occurs due to hydrodynamic forces (Walsh, 2013). Whereas local scour is the removal of sediment from the riverbed or seabed in the vicinity of the structure (Beg and Beg, 2013).

Scour formed when there are structures obstructing the flow pattern. Changes in flow characteristic in term of velocities may lead to changes in sediment transport capacity. This is due to the disequilibrium between actual sediment transport and the capacity of the flow to transport sediment. Scour will formed by adjustment of hydraulic condition in order to achieve new equilibrium (Hoffmans & Verheij, 1997).

Scour formation is related to the flow formation around the structure. The near-bed flows around pile that induce scour in wave condition are horseshoe vortex that formed at seabed and vortex shedding pattern at the lee side of pile (***Figure 2-1***).

The horseshoe vortex is caused by the incoming flow that rotating. This rotation happens in wave boundary layer when it is subjected to the waves.

If the wave boundary layer is too thin, this horseshoe vortex is insignificant. As the result from the interaction between two layers issuing from the side edges of the pile, the vortex shedding is formed (Williamson, 1985).

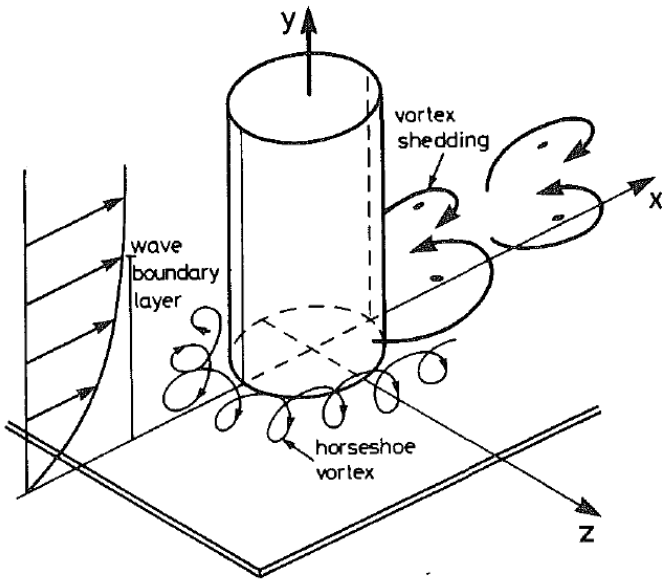

***Figure 2-1**: Near-Bed Flow around Pile. (Retrieve From: Sumer, Fredsøe and Christiansen. (1992))*

Beg et al. (2013) explained that process of scoring been affected by varies type of variables. For example pier, sediment characteristic and flow are the main role which affects the scouring time and spacing between piers.

Live-bed and the clear-water scour are two types of scour. Live-bed scour happens when there is carried away of bed material from the upstream reach into the crossing. The scour hole develops during the rising stage of a flood refills during the falling stage, which is a cyclic phenomenon (Walsh, 2013).

Clear-water scour occurs when there is no bed material being transported in the upstream reach is transported in suspension through the scour hole at the pier or abutment at less than the sediment transport capacity of the flow (Williamson,

1985). At the abutment or pier, the acceleration of the flow and vortices created by these obstructions cause the bed material around them to be transported.

During the incident of flood, bridges over streams with coarse-bed material are often exposed to clear-water scour at low discharges, live-bed scour at the higher discharges and then clear-water scour at the lower discharges on the falling stages (Beg and Beg, 2013). They further explained that clear-water scour needs more time to reach its utmost level than live-bed scour ***(Figure 2-2)***. This is due to clear-water scour occurs mainly in coarse-bed material streams. In fact, local clear-water scour may not reach a highest point until after several floods. Maximum clear-water pile scour is about 10 percent greater than the equilibrium live-bed pile scour.

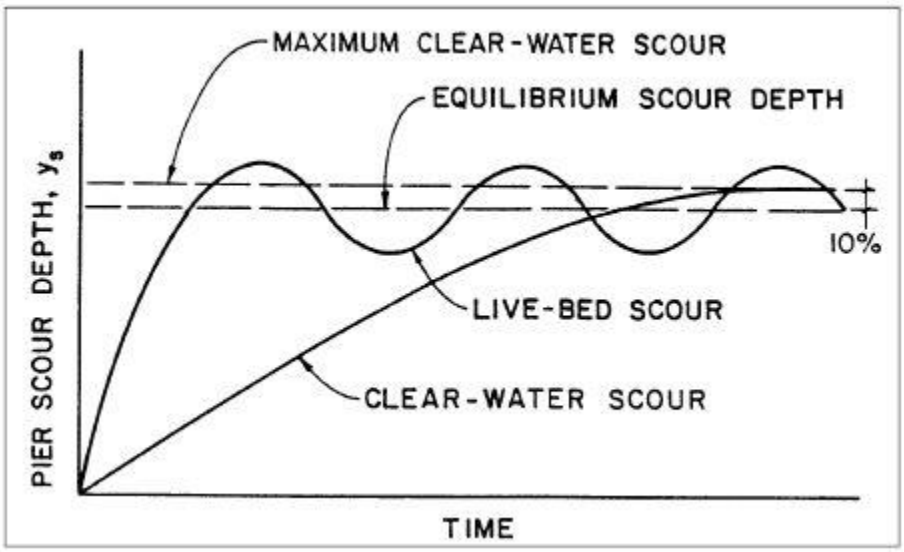

Figure 2-2*: Pier Scour Depth in a Sand-Bed Stream as a Function of Time. (Retrieve from: Beg and Beg, 2013)*

2.3 Typical Failures of Marine Structure due to Wave Scouring

Failure of marine structure is mainly due to continuous wave scouring at the toes. The failure is largely attributed to displacement of the marine structures, e.g. sliding, rotation of structure, overturning, tilting, and rotation ***(Figure 2-3)***.There will be a point where the scour formation becomes so deep that the foundation is been exposed, leading to unstable and lose of bearing condition, (Walsh, 2013).

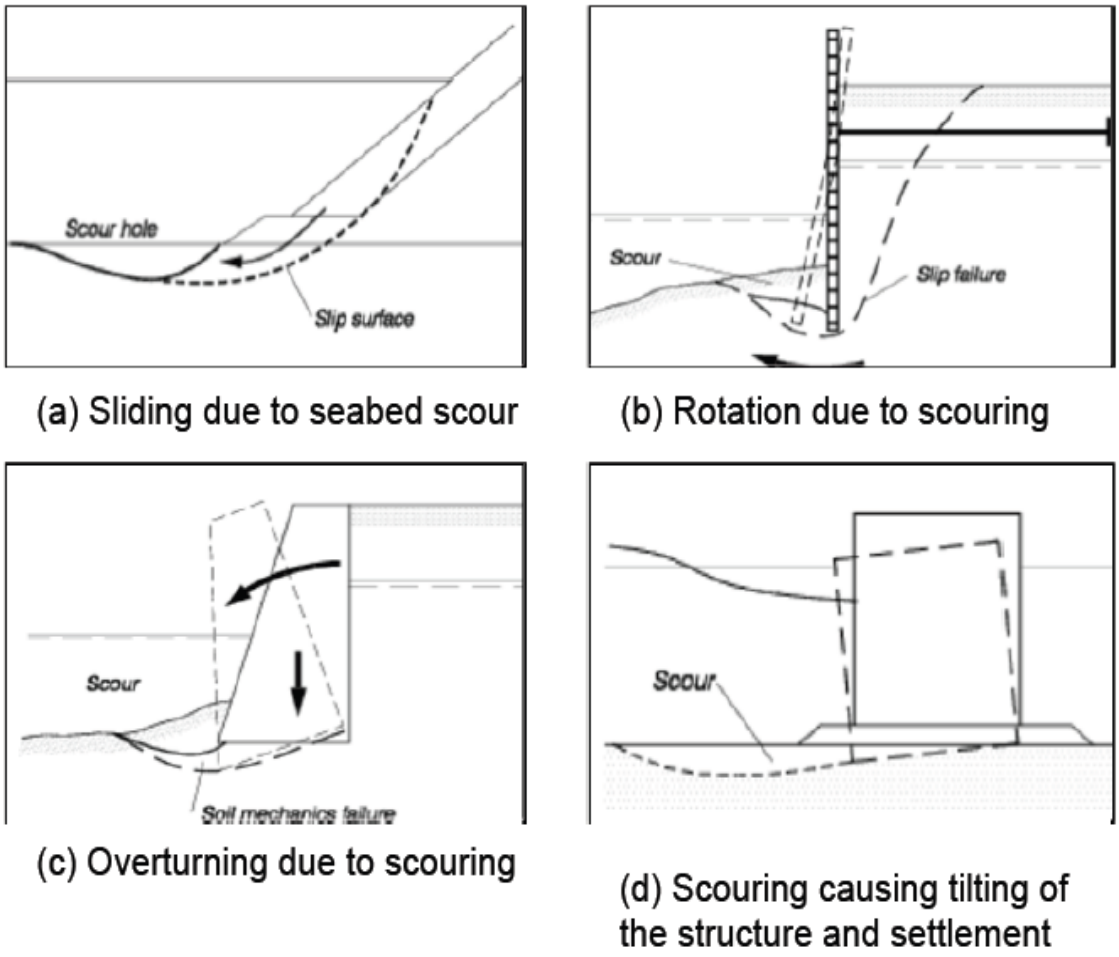

Figure 2-3*: Typical Failures Due to Wave Scouring (Retrieve from: Walsh , 2013)*

Walsh (2013) elaborated that failure of structure in ***Figure 2-3 (a)*** shows formation of scour hole close to the foot of the structure is due to wave. The toe functions as support for the main armour. Thus, erosion at the toe causes undermining of the armour. This eventually reduces the stabilizing forces causes slip failure to occur which results in sliding of armour. Whereas is ***Figure 2-3 (b)*** erosion at the toe eliminates the passive pressure from the soil. Subsequent rotation of the wall occurs when loads from the active soil pressure and the pressure from the groundwater exceeds the passive pressure (Walsh , 2013).

Scour infront of the wall reduces the passive resistance and the bearing capacity of the foundation soil (***Figure 2-3(c)).*** The resulting load from the active backfill pressure, the high groundwater table and the weight of the wall causes bearing capacity failure in the soil resulting in a foreward overturning and some settlement of

the wall (Walsh, 2013). Lastly in ***Figure 2-3 (d)*** shows failure of structure when formation of scour in front of a caisson due to wave might cause seaward tilt and settlement of the caisson. The critical wave load situations are when deep wave troughs occurs at the caisson front (Walsh , 2013).

2.4 Formation of scour around a vertical pile in waves

Sumer et al. (1992) conducted an experiment to analyse the formation of scour were around vertical pile subjected to waves. Three types of wave flume of different size were used with different sediment grain sizes and diameter sizes of pile. Scour depths were measured at four points near the pile structure, i.e. upstream of pile, downstream of pile and two side edges of pile.

From their finding, scour hole had a shape of a truncated cone. The equilibrium scour depths were obtained when the sediment transport in the scour hole were equal to the sediment transport far from the pile. In case of live-bed where sediment transports were in motion, the variations of scour depth with shield parameter were week. They also found that Re number was depend on the surface roughness of pile where the vortex shedding patterns were affected.

From the observation, the shed vortex acted like a cyclone that sweeping the sediment grains into its core region. Then, the grains were lifted into the upper portion of the vortex by the updraft. On other hand, horseshoe vortex was effective in eroding the bed at the upstream of the pile. It might be expected that the KC number had influenced in the formation of scour by shed vortex for small KC value and horseshoe vortex for large KC value. They had developed an equation that show the relationship of the equilibrium scour depth with KC number based of graph plotted (***Figure 2-4***).

They concluded that scours were form by the formation of horseshoe vortex and lee-wake vortices around a pile. KC number was a main parameter in determine the equilibrium scour depth where the most of scour data in this experiment was on live bed only.

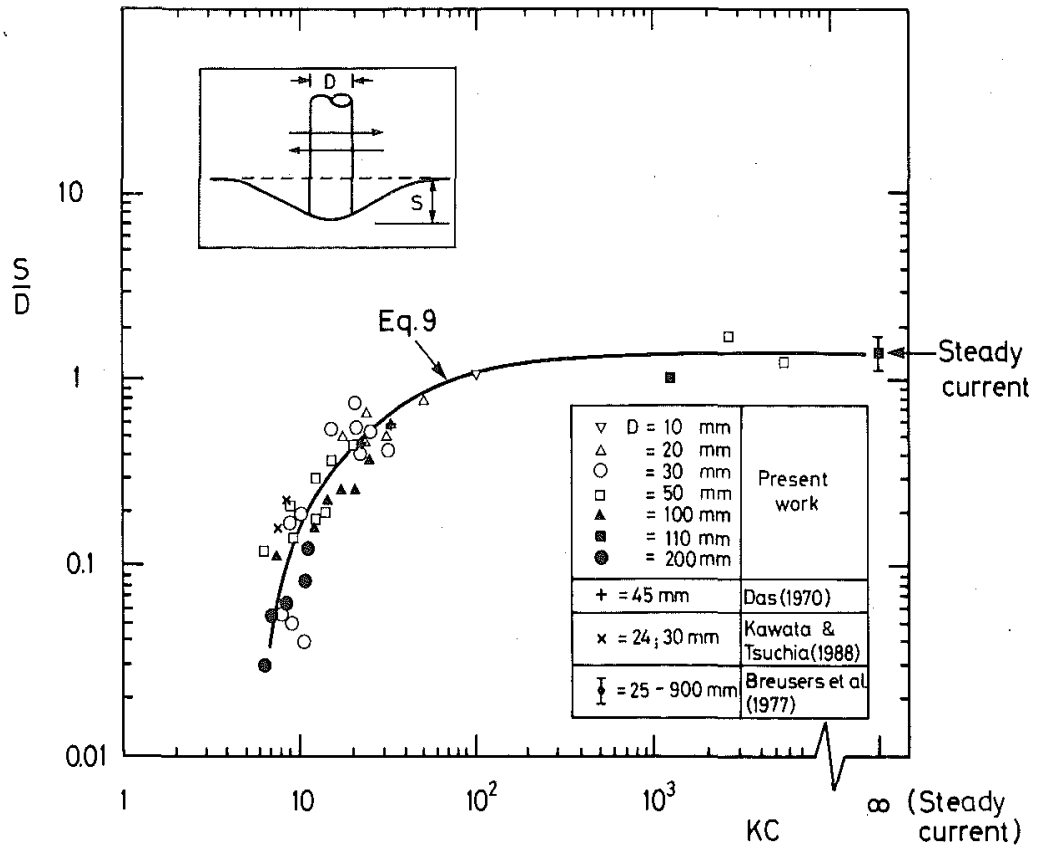

***Figure 2-4**: Equilibrium Scour Depth versus KC Number. Live Bed ($\theta > \theta_{cr}$). (Retrieve from: Summer et al. (1992))*

Sumer et al. (1993) investigated the influence of cross-sectional shape on the scour depth. The result showed that the cross section has significant effect for small values of KC number. ***Figure 2-5*** and ***Figure 2-6*** shows their finding where the scour depth was largest for cross section of the critical value of KC was smallest which 45° square pile is. It is smallest for the cross section where the critical value of KC was large which 90° square pile is. From ***Figure 2-6***, when KC increased, the differences between the three different piles cross section become relatively smaller.

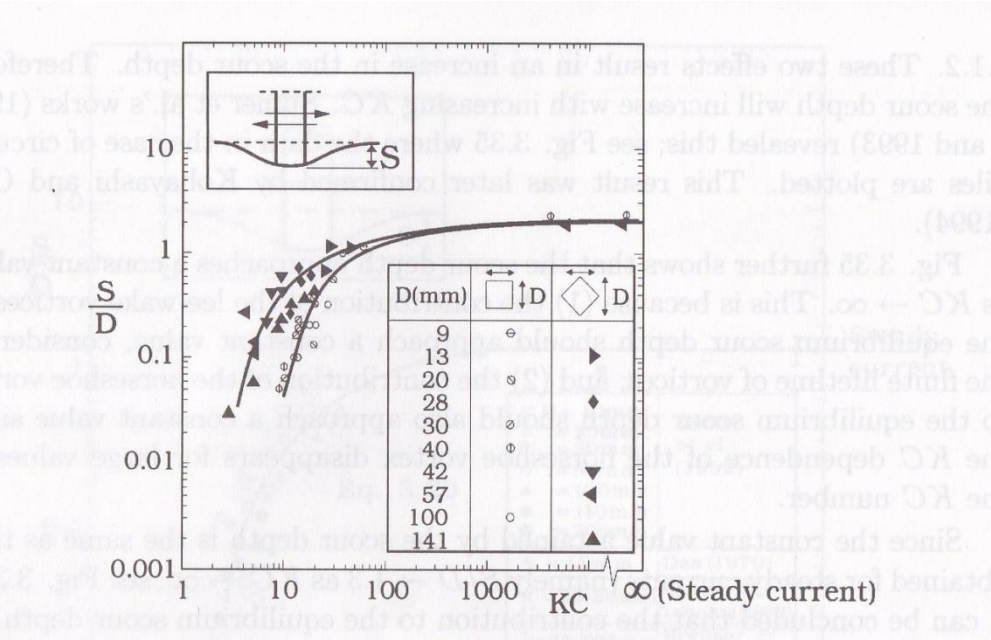

Figure 2-5: *Equilibrium Scour Depth For Square Pile In Live Bed. (Retrieve From: Sumer et al. (1993)*

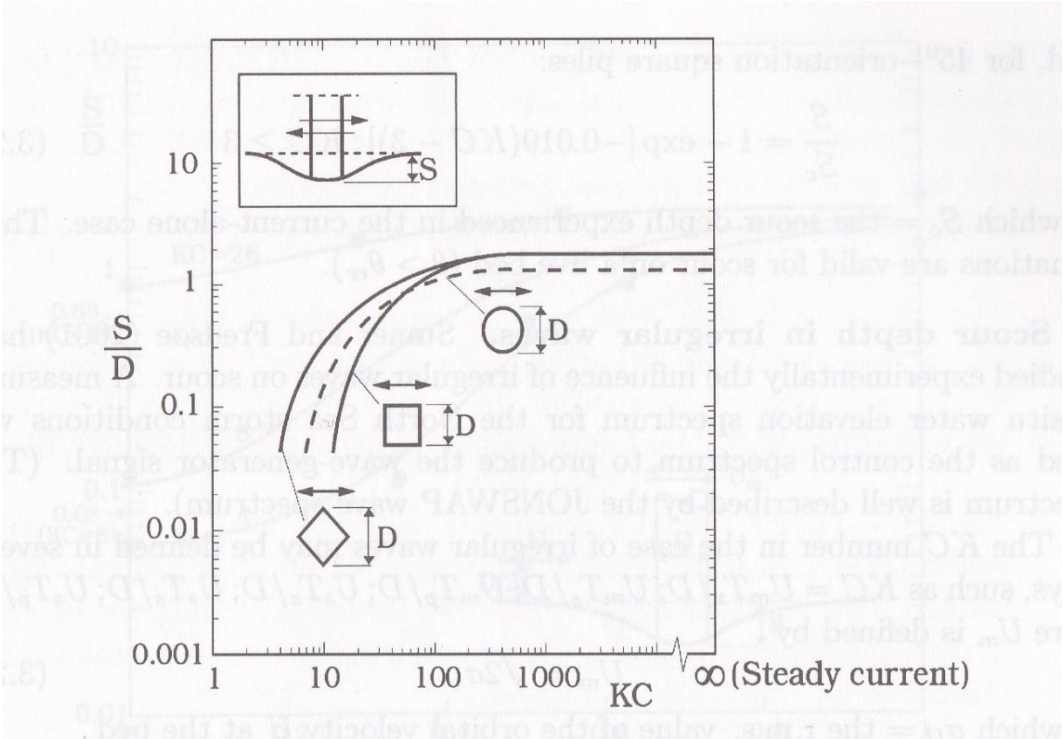

Figure 2-6*: Effect of Cross-Sectional Shape to the Equilibrium Scour Depth for Live Bed. (Retrieve From: Sumer et al. (1993)*

Scour depth prediction using numerical method also had been studies by Myrhaug and Rue (2003). ***Figure 2-7*** until ***Figure 2-8*** shows their result to present an approach for deriving scour depth around vertical pile with comparison data from Sumer et al. (1992). The data show that stochastic approach for s1/10 and E(s1/10) which describe probability number of random wave were close to Sumer and Fredsoe model for large KC_{rms} value and the both result for circular and square were almost coincide. They had concluded that $1/10^{th}$ probability values (10^{th} highest wave height) agree very well with model for random wave scour.

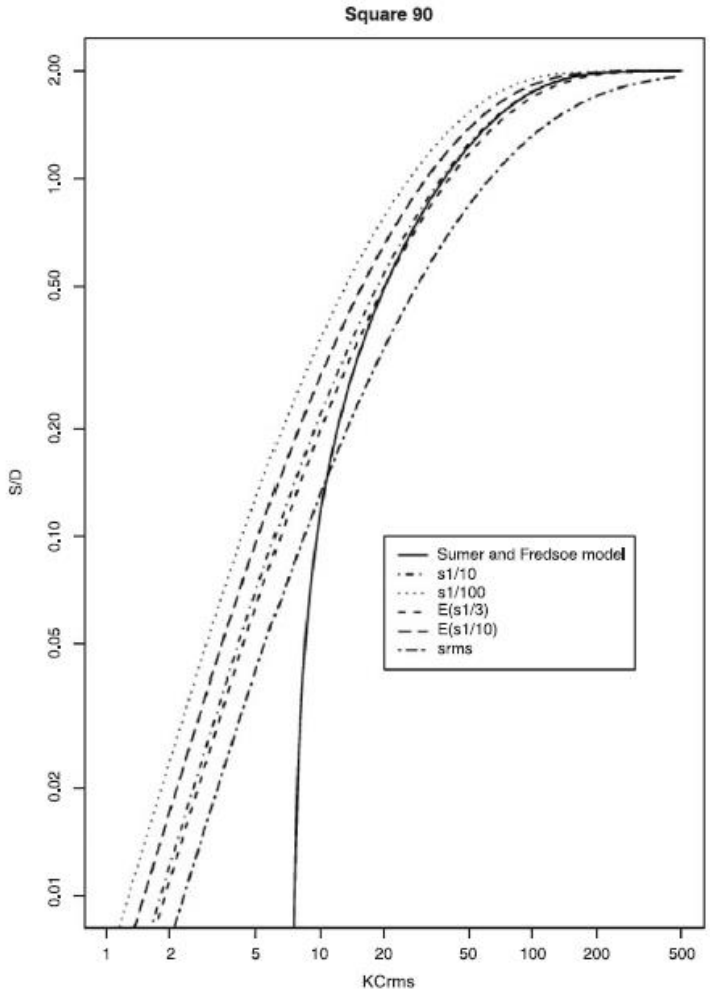

Figure 2-7: *Prediction for Irregular Waves of S/D versus* Kc_{rms} *for Scour around Vertical Square Pile with 90° Orientation. (Retrieve From: Myrhaug and Rue (2003))*

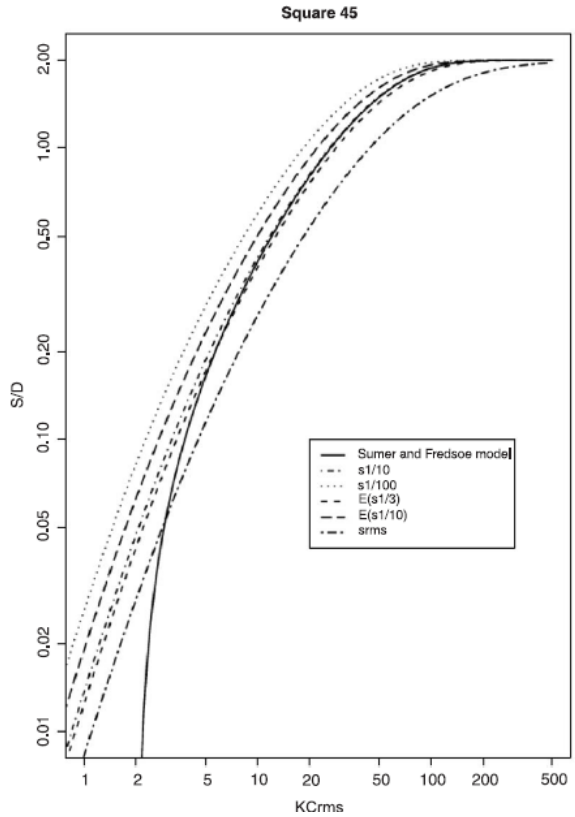

***Figure 2-8**: Prediction for Irregular Waves of S/D Versus Kc_{rms} for Scour Around Vertical Square Pile with 45° Orientation. (Retrieve From: Myrhaug and Rue (2003))*

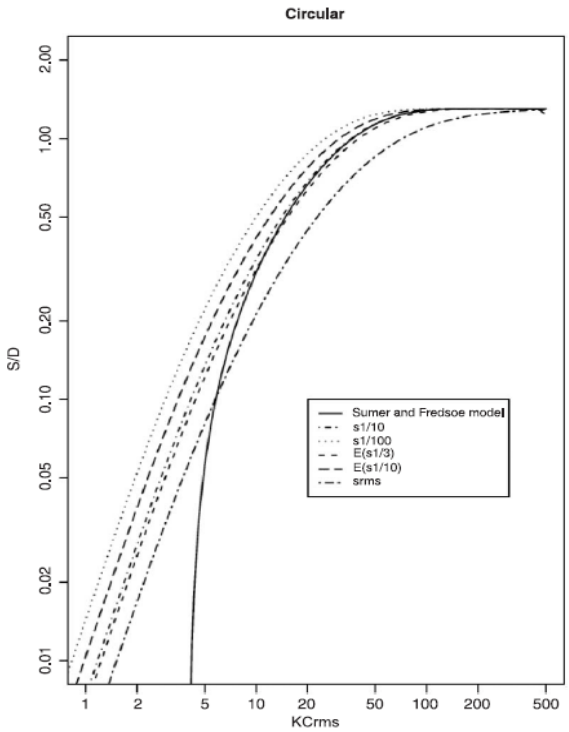

***Figure 2-9**: Prediction for Irregular Waves of S/D Versus Kc_{rms} for Scour around vertical Circular Pile. (Retrieve From: Myrhaug and Rue (2003))*

Sumer and Fredsøe (2001) investigated the wave scour around large vertical circular cylinder to stimulate for platform leg structure. The physical model was setup with subjected to regular wave condition. They observed that the scour or erosion process was continuing and streaming may cease to exist when the scour position process attains its equilibrium state. The scour depth also observed able to reach about 4% of the diameter of structure.

Figure 2-10 shows the KC number and diffraction parameter, D/L was affect the equilibrium scour depth. Scour depths were increase and the KC and D/L were increased where it corresponding to large steady streaming. However, data collapse for further increase in D/L where it may be linked with the decrease in the phase-resolved velocity for very large values of D/L.

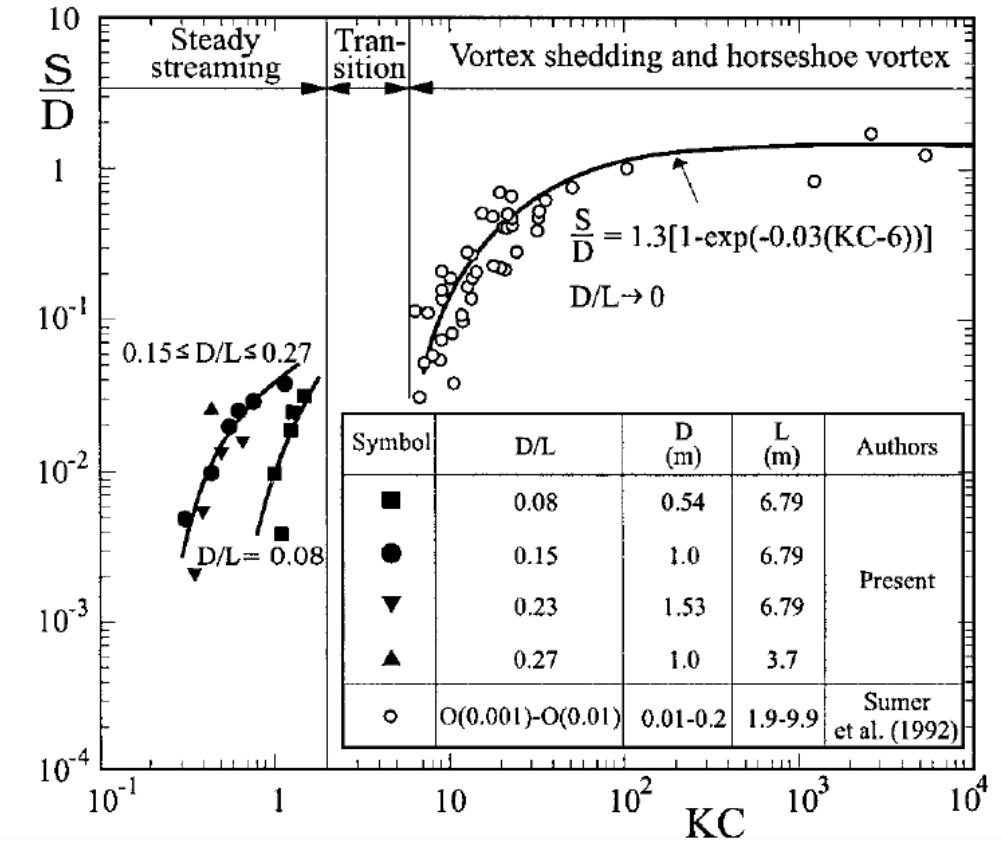

Figure 2-10*: Maximum Scour Depth at Periphery of Cylinder Base in Live Bed with Comparison from Summer et al. (1992) Data. (Retrieve From: Sumer and Fredsøe (2001))*

2.5 The effect of sediment condition on wave scour around a pile

Sediment condition around pile will affect the scour formation. Sumer et al. (2007) investigated on wave scour around a circular pile in three kinds of soil which are dense silt, medium dense silt, and sand under uniform regular waves. They observed that scour begin to occur after liquefaction or compaction process which is large wave height able to liquefy the soil. ***Figure 2-11*** shows the effect of KC number to equilibrium scour depth with different sediment condition. The onset of net scour was directly related to the lee wake vortex flow for small KC number and horseshoe vortex predominately for large KC value. Scour depth also depend on the relative density of sediment where scour increase as relative density increase together with friction angle. The time scale for scour equilibrium in medium dense silt was took relative larger than sand.

For Shield parameter effect the scour depth, the range of the Shield parameter in this experimental for sand data does not extend so as to cover the values of the Shield parameter for dense-silt test as shown in ***Figure 2-12***. There no study yet to investigate the influence of shield parameter on scour in waves in systematic manner.

Symbol	Soil	Relative density D_r	Shields parameter θ
●	Dense silt	0.73	0.3-0.6
o	Loose silt	0.38	0.2-0.4
Δ	Sand	0.23	0.2-0.3

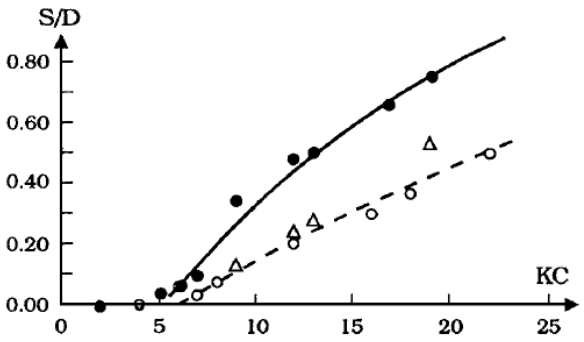

Figure 2-11: *Equilibrium Scour Depth at the Pile Normalized by the Pile Diameter as a Function of Kc Number. (Retrieve From: Sumer et al. (2007))*

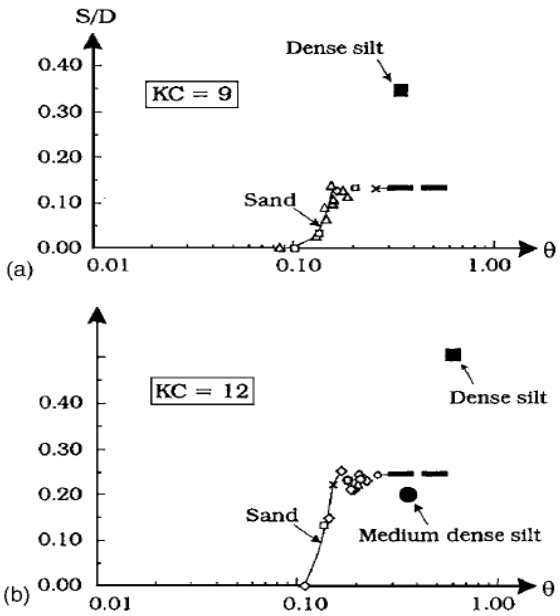

Figure 2-12: *Equilibrium Scour Depth at the Pile Normalized by the Pile Diameter as a Function of Shield Parameter. (Retrieve From: Sumer et al. (2007))*

To study the effect of pile driven in soil, two piles was use in this experiment. First pile was initially installed in silt and subjected to wave flow until liquefaction process is ended. Then, the second pile was driven installed in dense silt and both were continue subjected to wave flow until they achieved equilibrium scour depth. The measured scour depth around both pile were same which show the density of the silt around the second pile was practically same as that of the rest of the soil.

From this study, they concluded that scour depth in wave influence by relative density, shield parameter and KC number. Scour depth independent from Shield parameter when Shield parameter was larger than critical value to cause suspension of sand at sides of pile. However, the data were quite limited.

Dey et al. (2011) conducted a study to determine the equilibrium scour and time variation of scour depths at circular piles embedded vertically in clay alone and sand-clay mixed beds under monochromatic waves. ***Figure 2-13*** show the variation of equilibrium scour depth with KC for different n value which is describe percentage of clay proportion in sand (e.g.: n =0.3 means 30% clay, 70% sand). The reduction of scour depth was evident with an increase of clay portion. This is because the erodibility of the sediment where the same vortices cannot erode the bed in the far field when clay proportion was increased.

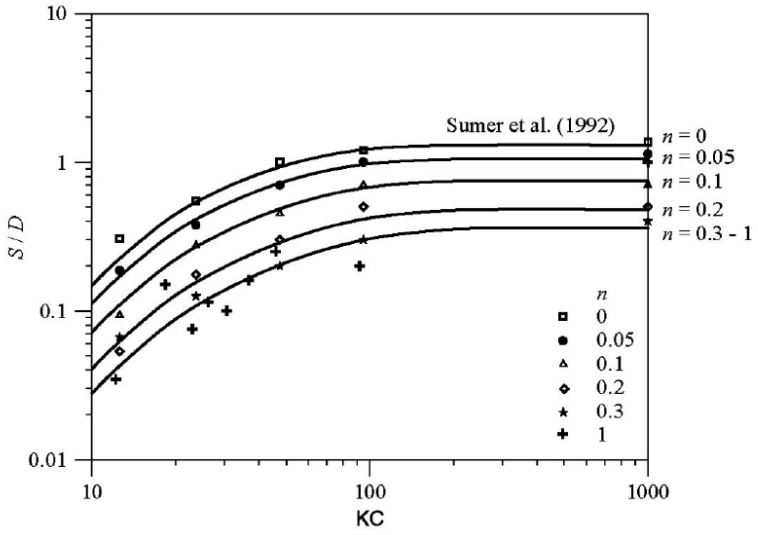

***Figure 2-13**: Variation of Equilibrium Scour Depth with Kc for Different N Value. (Retrieve From: Dey et al. (2011))*

Figure 2-14 shows that the equilibrium scour depth with time for different KC in n =1. The scour depths were developed over a long period of time to achieve an equilibrium scour depth even the scour depth was small; the time scale to reach equilibrium was quite long. Further research shall be conducted by focusing on time variation of scour for more KC number with variation of clay proportion.

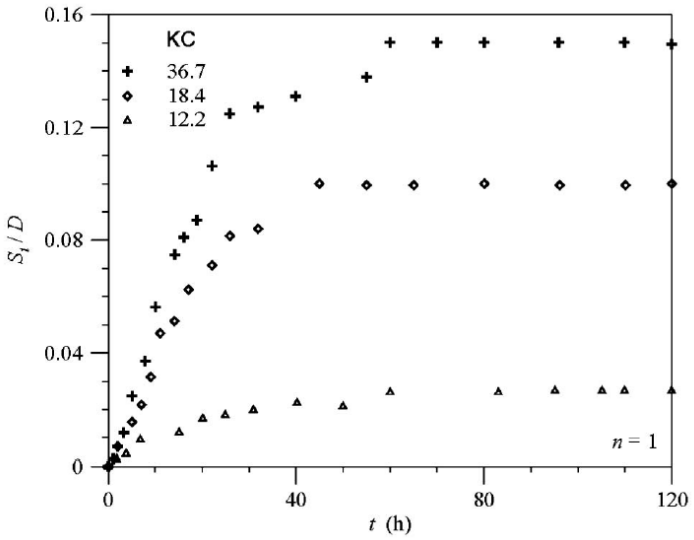

***Figure 2-14**: Variation of Equilibrium Scour Depth with Function of Time for Different Kc Value. (Retrieve From: Dey et al. (2011))*

They concluded that equilibrium depth at pile will reduced with increase of clay proportion in sand-clay mixture. The scour depth reduced for n = 0.3 and 1 are

almost equal. The timescale of equilibrium scour depth was increased as the KC number was increased.

2.6 Empirical Formulation for Scour Evaluation

Sumer, Fredsøe and Christiansen (1992) proposed the following empirical expression for determination of the scour depth, S, equilibrium at a vertical pile of diameter, D (***Figure 2-15)*** exposed to regular wave condition:

$$\frac{S}{D} = C(1 - exp[-q(KC - r)]) \quad for\ KC \geq r \tag{2.1}$$

where C, q and r are coefficients given by the following values:

for circular pile {C, q, r} = {1.3, 0.03, 6},

square pile 90^o orientation {C, q, r} = {2, 0.015, 11},

square pile 45^o orientation {C, q, r} = {2, 0.019, 3}

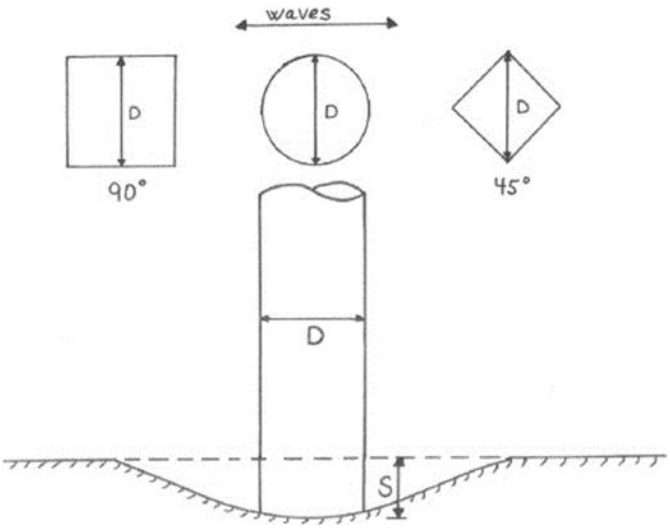

Figure 2-15*: Definition Sketch Of The Scour Depth (S) Around A Circular Vertical Pile With Diameter (D). (Retrieve From:Myrhaug & Rue,2003)*

The Keulegan-Carpenter (KC) number is main factor for the vortex shedding pattern in oscillatory flows (Williamson, 1985; Sumer et al. 1992). The Keulegan-Carpenter (KC) number is a dimensionless parameter where comparing the amount drag forces over inertia forces for object in an oscillatory fluid flow. For wave flow pattern condition, the KC number is defined by

$$KC = \frac{U_m T}{D} \tag{2.2}$$

where $\mathbf{U_m}$ is the undisturbed linear near-bed orbital velocity amplitude and **T** is the wave period. Scour becomes in appreciable at KC < 6, (Ong, Myrhaug and Hesten, 2013)

Equations (2.1) and (2.2) are valid for live-bed scour, for which θ > θcr where θ is the undisturbed Shields parameter defined by

$$\theta = \frac{\tau_w}{\rho g (s-1) d_{50}} \tag{2.3}$$

where $\boldsymbol{\tau_w}$ is the maximum bottom shear stress under the waves, **ρ** is the density of the fluid, **g** is the acceleration due to gravity, **s** is the sediment density to fluid density ratio, $\mathbf{d_{50}}$ is the median grain size diameter, and **θcr** is the critical value of the Shields parameter corresponding to the initiation of motion at the bed. One should note that the scour process will attains its equilibrium stage through a transition of period.

The maximum bottom shear stress within a wave cycle is taken as:

$$\frac{\tau_w}{\rho} = \frac{1}{2} f_w U^2 \tag{2.4}$$

where $\boldsymbol{f_w}$ is the friction factor and is valid for waves plus current for wave-dominated situations.

$$\boldsymbol{f_w = c\left(\frac{A}{Z_0}\right)^{-d}} \tag{2.5}$$

{c, d} = {18, 1} for $20 < \frac{A}{Z_0} < 200$,

{c, d} = {1.39, 0.52} for $200 \leq \frac{A}{Z_0} < 11000$,

{c, d} = {0.112, 0.25} for $11000 \leq \frac{A}{Z_0}$

where **A=U/ω** is the near-bed orbital displacement amplitude, **ω=2π/T** is the angular wave frequency, and $\mathbf{Z_0=d_{50}/12}$ is the bed roughness. Ong, Myrhaug and Hesten (2013) also further added that the KC number can alternatively be expressed as:

$$\boldsymbol{KC = \frac{2\pi A}{D}} \tag{2.6}$$

A from equation (2.6) can be related to the linear wave amplitude a by:

$$\boldsymbol{A = \frac{a}{\sinh kh}} \tag{2.7}$$

where **h** is the water depth, and **k** is the wave number determined from the dispersion relationship $\boldsymbol{\omega^2=gk \tanh kh}$.

2.7 Countermeasures for Scour Reduction

One of the important design criteria of marine structure is to reduce scour holes such that the foundation bed is not exposed (Walsh, 2013). Beg et al. (2013) explained by using flow altering mechanism, the shear stresses on the seabed, in vicinity of pier are reduced because the flow pattern around a pier been altered thus reduces the scour depth. Some flow-altering countermeasures used against scour problem at marine structure are discussed in the following section.

2.7.1 Splitter Plates

These plates are placed such that they simply divide the flow of water, causes disruption of flow pattern, therefore reducing the effects of vortex shedding (Walsh, 2013). Dey, Sumer and Fredsøe (2006) explored on the reduction of scour at vertical piles under monochromatic waves by using splitter plates. They conducted experiment in a wave flume by using pile diameter of 4 and 6 cm with water depth was maintain constant 0.4m. ***Figure 2-16*** shows the splitter plate used which is 0.45m wide and attached vertically to the pile facing the flow.

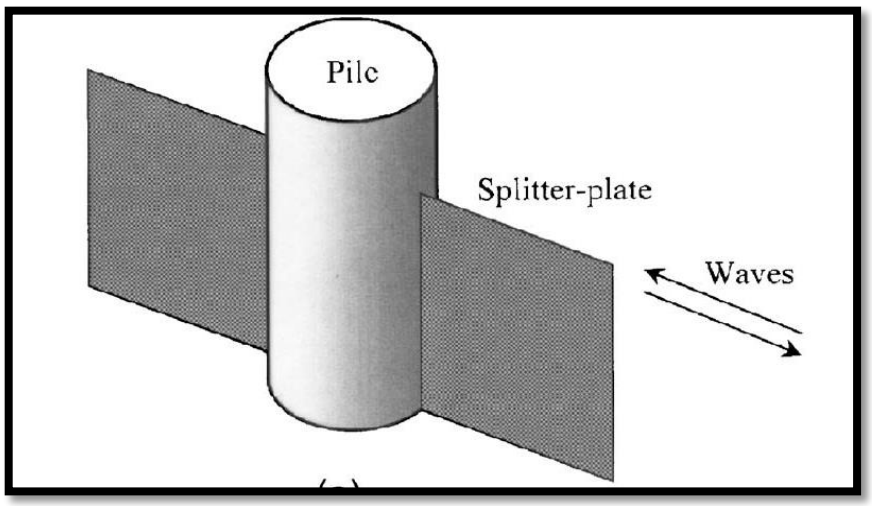

Figure 2-16*: Spiltter Plate Attached To The Pile Along The Vertical Plane Of Symmetry. (Retrieve From: Dey, Sumer and Fredsøe, 2006)*

They have concluded that the average reduction of scour around pile compared to unprotected pier with the use of splitter was 61.6%. ***Figure 2-17*** shows the experimental results of unprotected and protected pile correspond with the curve proposed by Sumer et al. (1992). Here, the reduction of scour is prominent as the data plots are below the curve.

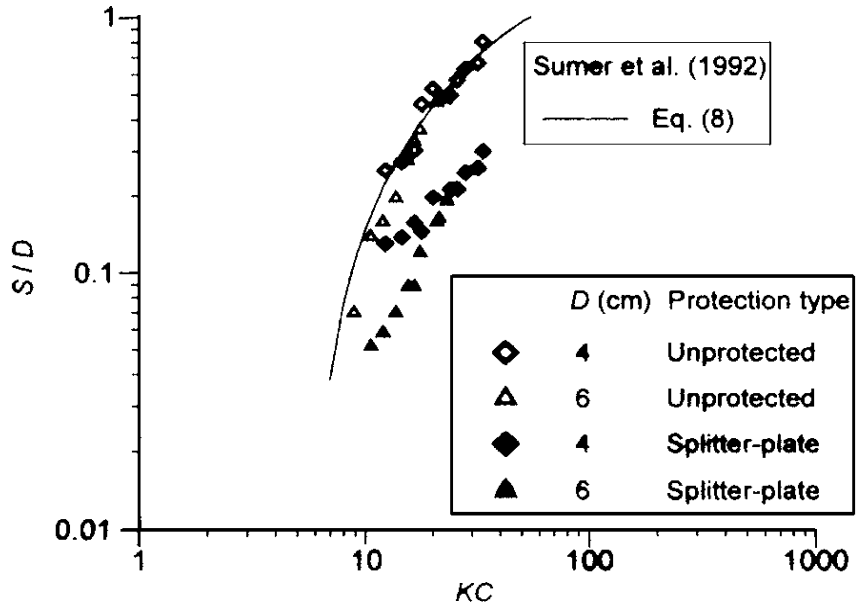

Figure 2-17: *Variation of Nondimensional Scour Depth S/D with Kc for Splitter Plate as Protection. (Retrieve From: Dey, Sumer and Fredsøe, 2006)*

2.7.2 Slots

Slots will relapse the water flow to reduce scour depth. Sizes of slots depend on the water conditions (Walsh, 2013). Ali, Roberto and Francesco (2012) conducted experiment using slot as countermeasure which was performed in clear-water condition with flow intensity slightly below the threshold of sediment motion. They have run four test series of different slot length, l_s (***Figure 2-18***) using 4cm diameter, *d* and 10cm height, *h* pile.

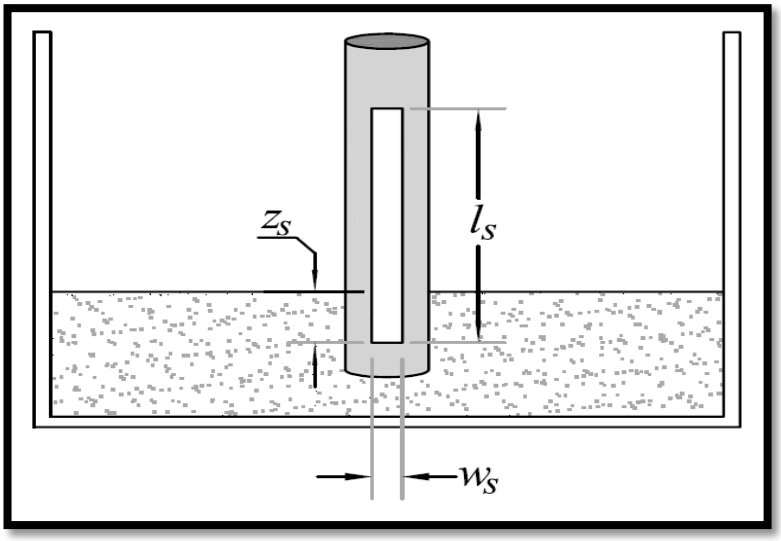

Figure 2-18: *Flow-Altering Countermeasures: Pier Slot (Retrieve From: Ali, Roberto and Francesco, 2012)*

The results and configuration of their experiment for test B5 to B8 showed in ***Figure 2-19*** where it was compared with unprotected pile, B0 with scour depth, d_{se} of 7.62cm. The results shows that test series B8 gives the best scour depth reduction which is 35% while in test B5 with shorter slot length the efficiency reduced is only about 2%. They have concluded that the slot length and location for obtaining maximum efficiency is by using optimum slot configuration which is $l_s = h/2 + 0.7d_{se}$.

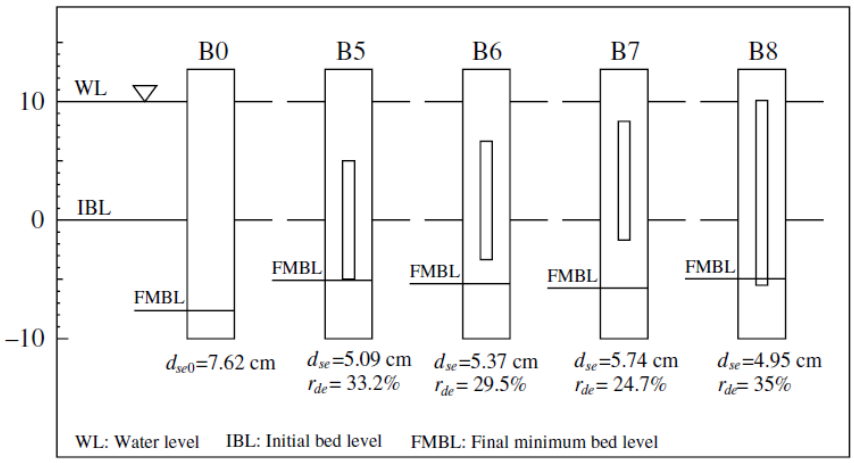

Figure 2-19*: Configurations and Results Of Tests B0 And B5 To B8 (Units: Cm) (Retrieve From: Ali, Roberto and Francesco, 2012)*

2.7.3 Collars

This technique is commonly used to reduce local scouring effects by redirecting the flow to protect the structure from direct impact of water. Collars are known to be more effective and efficient for water flowing around rectangle objects (Walsh, 2013). Ali, Roberto and Francesco (2012) performed experiment using collar ***Figure 2-20*** as countermeasure which was conducted in clear-water condition with flow intensity slightly below the threshold of sediment motion. They used 3*b*-wide, 5mm thick transparent Perspex collar flush, and h_c = 10cm. The pier used was 4cm in width, *b*. and 10cm in height, *h*. Basically the selected this parameters to obtain the maximum possible efficiency of a practical collar size. They have compared the results to scour depth of unprotected pier and found that the scour reduction was equal to 28.7%. Collar has been clarify as a mechanism that slows down scour rate, thus tests associated with collar should be longer compared to unprotected pile to achieve the equilibrium state (Ali et al. 2012).

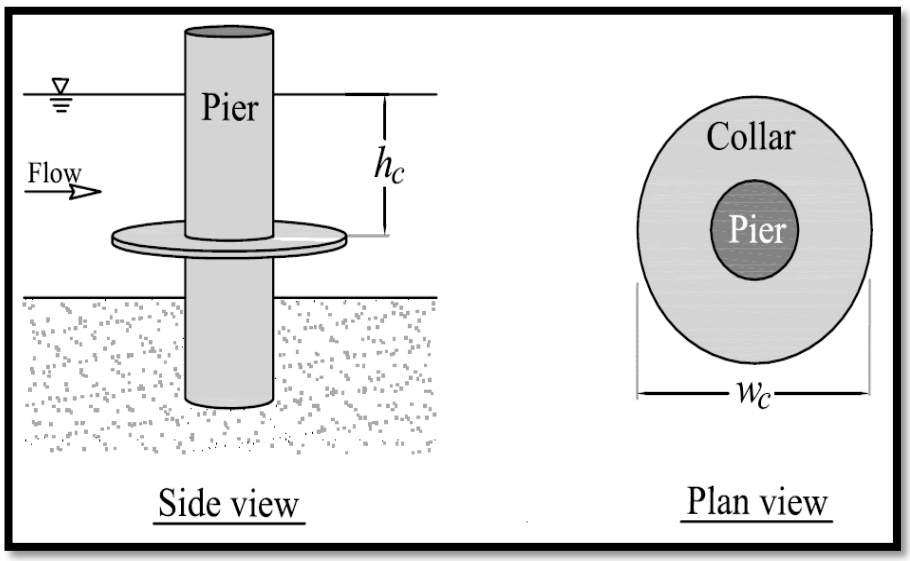

Figure 2-20*: Flow-Altering Countermeasures: Collar (Retrieve From: Ali, Roberto and Francesco, 2012)*

2.7.4 Threaded Piles

The threads on the pile cause the correction in flow to disrupt the usual frequency pattern of vortex shedding, (Sumera nd Fredsøe, 1997). Dey, Sumer and Fredsøe (2006) conducted experiment to test the efficiency of threaded pile in reducing scour depth. The experiment was conducted for single threaded pile ***(Figure 2-21)*** with helical wire diameter of 2 and 3 cm wrapped spirally. The pile diameter 4 and 6 cm was used with thread angle of 65^o and 60^o respectively.

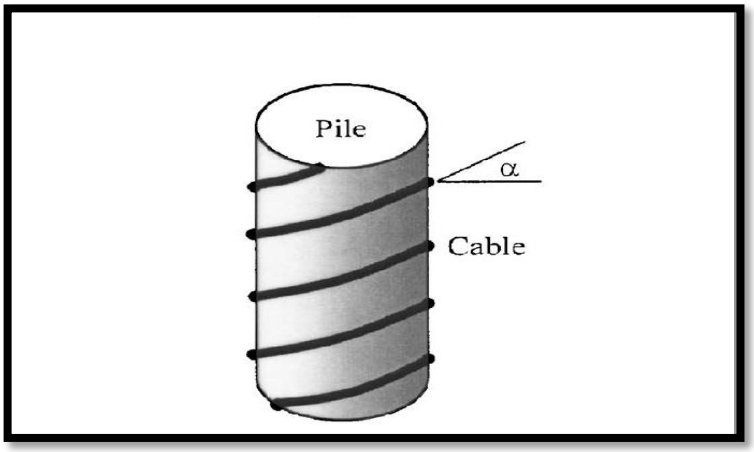

Figure 2-21*: Threaded Pile (Helical Wires Wrapped Spirally on the Pile to form Thread (Retrieve from: Dey, Sumer and Fredsøe, 2006)*

The results was compared with scour depth of unprotected pier where it shows that for cable size 3cm using 4cm and 6 cm pile diameter obtained average scour reduction of 51.1% and 48.1%. Whereas for cable size 2cm with pile diameter of 4cm and 6cm shows average scour reduction of 48.1% and 43.2%. Dey at al. (2006) showed the comparison of Sumer et al. (1992) curve with their experimental results **(*Figure 2-22)***. They further explained that there is biological growth takes place in the marine atmosphere gradually cover up the piles and wrapped wires are Thus, there is a possibility after a few years that the protection device becomes less effective.

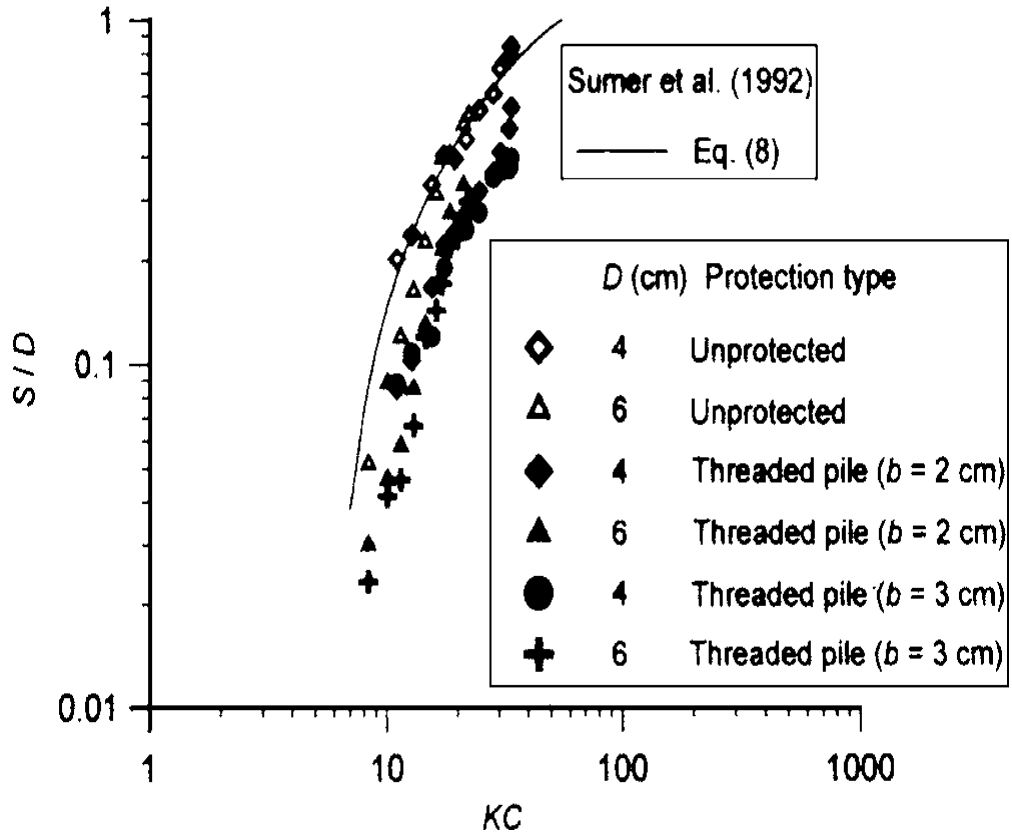

***Figure 2-22**: Variation of Nondimensional Scour Depth S/D with Kc for Threaded Pier as Protection . (Retrieve From: Dey, Sumer and Fredsøe, 2006)*

2.8 Concluding Remark

In order to improve previous research, certain parameters had been looked for identifying research gap between them before conducting the experiment. By relating to the topic, parameters considering in this study are the flow-altering countermeasures, flow condition, material of sediment, and the pile size. Specifically, Dey et al. (2006) conducted experiment on using double and triple thread pier as flow-altering countermeasures and produced results based of percentage of scour reduction. Scour protection using cross-threaded pier has never been explored. Thus in this study, experiment on cross-threaded pier will be conducted to compare the efficiency of reducing scour depth around pier with previous research results.

CHAPTER 3
METHODOLOGY

3.1 Introduction

This research involves a physical modelling was carried out in the Hydraulics Laboratory of University Technology of Petronas. A well-prepared experimental set-up is essential in ensuring the quality of the experimental results obtained. The laboratory experiments were conducted in a controlled environment whereby tides, currents and wind will not be taken into consideration. The waves were generated in the wave flume for the experiment was monochromatic and regular waves. The tests of different series were conducted to measure the performance of different innovative scour countermeasure. Two types of models which are single cross-threaded piers and double cross-threaded piers were tested with different configuration of thread angle and cable diameter. The procedure and equipment used in this experiment will be explained in detail in this chapter. The measured parameter done in this study to measure the performance of models mainly the scour depth of model to scour depth of model without protection.

3.2 Model Scaling

A 30 mm diameter pier was installed in sand middle of the flume. To neglect flume sidewalls effect on to the scour depth, the pier diameter selected should be less than 10% of the flume width, (Chiew and Melvill,1998; Izadinia and Heidarpour, 2012). In this experiment, the pier diameter is about 9.9 % of the flume width.

In order to avoid the effect of the sediment size to the scour depth, the pier diameter to the median grain size (D/d_{50}) should more than 50 (Chiew and Melville, 1987; Izadinia and Heidarpour, 2012). In this experiment, sand sediment with d_{50}= 0.48 mm was used as ***Figure 3-1*** shows the particle distribution size of the sediment. The pier diameter to the median grain size (D/d_{50}) is 62.5 which is well beyond 50. Therefore, this scale effect can be eliminated from the study.

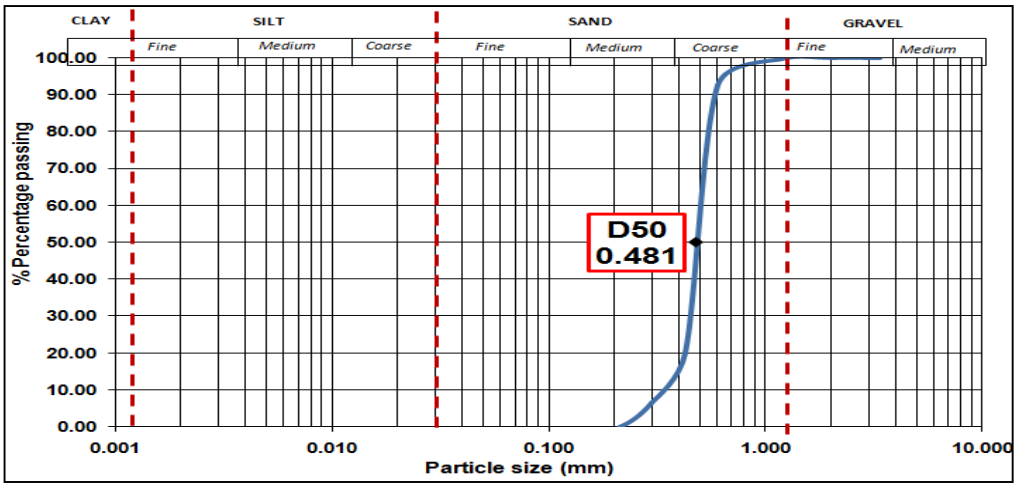

***Figure 3-1**: Particle Distribution Size of the Sediment*

3.3 Test Model

Four two of models have been selected, i.e. (a) cross thread cable and (b) double cross thread cable as shown in ***Figure 3-2***. The thread angle and cable diameter used for both cross-threaded piers are varying which are 15° and 30°, and 2 mm and 3mm respectively. ***Table 3-1*** shows the properties of the test model used in this experiment.

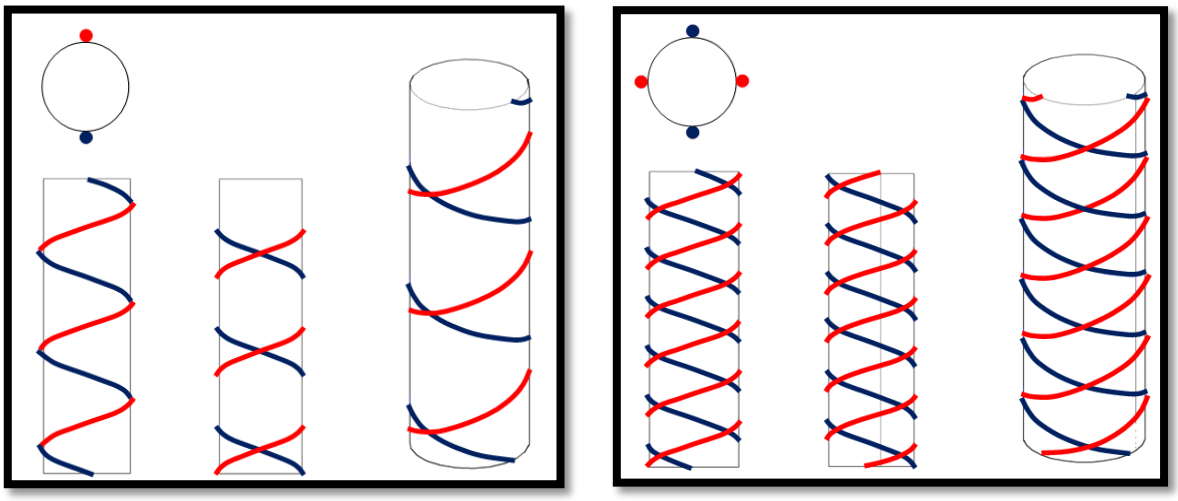

(a) (b)

***Figure 3-2**: Test models; (a) single cross thread cable, (b) double cross thread cable,*

***Table 3-1**: Summary of experiment*

Type of Pier	Thread angle, θ	Cable diameter (b, mm)
Single pier without protection	-	-
Single cross threaded pier	15°, 30°	2, 3
Double cross threaded pier	15°, 30°	2, 3

3.4 Project Activities

The series of tests were conducted in an open channel flume at the Hydraulic Laboratory of UTP. The dimension of the flume is 32 cm width, 10 m length and 48 cm height shown in ***Figure 3-3***. The regular wave generated by the wave paddle which is connected to a motor and can be controlled using valve as shown in ***Figure 3-4***. All electrical switching units required for operations are located in the cover of the switch box as shown in ***Figure 3-5***. A kind of absorber was placed at the upstream of flume used to minimise unwanted reflections of wave energy that compromise test results shown in ***Figure 3-6***. The test was conducted in 1s of wave period, T which will be using empirical formula as shown in ***Table 2***.

***Table 3-2**: Formula for Period (Cycle Duration), T*

Physical value	symbol	unit	abbreviation	formula
Cycle duration	$T = 1 / f$	**second**	**s**	$T = \lambda / c$
Frequency	$f = 1 / T$	**hertz**	**Hz = 1/s**	$f = c / \lambda$
Wavelength	λ	**Meter**	**m**	$\lambda = c / f$
Wave speed	c	**meter per second**	**m/s**	$c = \lambda \times f$

The period of a wave is the time for a particle on a medium to make one complete vibrational cycle. Point gauge that will be placed at the top of flume is for measuring the scour depth as shown in ***Figure 3-7***. The reading of point gauge in this experiment will be done precisely in one decimal place with unit of centimetre.

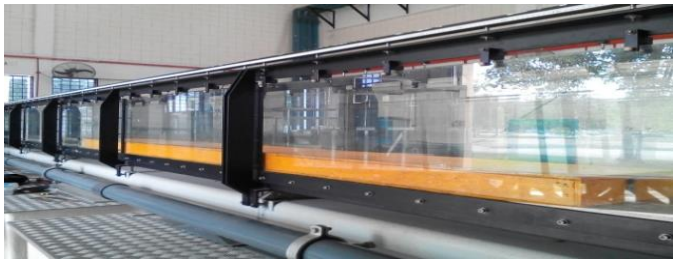

***Figure 3-3**: Open channel flume*

Figure 3-4: *Wave Paddle*

Figure 3-5: *Switch Box*

Figure 3-6: *Wave Absorber*

Figure 3-7*: Point Gauge*

3.5 Laboratory Set-up

The pier will be located at the mid-length of the flume. The 3 m of false floor was located at upstream as shown in ***Figure 3-8*** of pier followed by 3m of sand with depth of 10 cm illustrated in ***Figure 3-9***. Before the sand sediment was inserted in the flume, 3.5 m long of goetextile was laid down on the flume bed as shown in ***Figure 3-10*** Lastly, 1 m of buffer zone was set-up at the end of flume followed by the wave paddle to generate wave. The complete set-up of the flume is shown in ***Figure 3-11***.

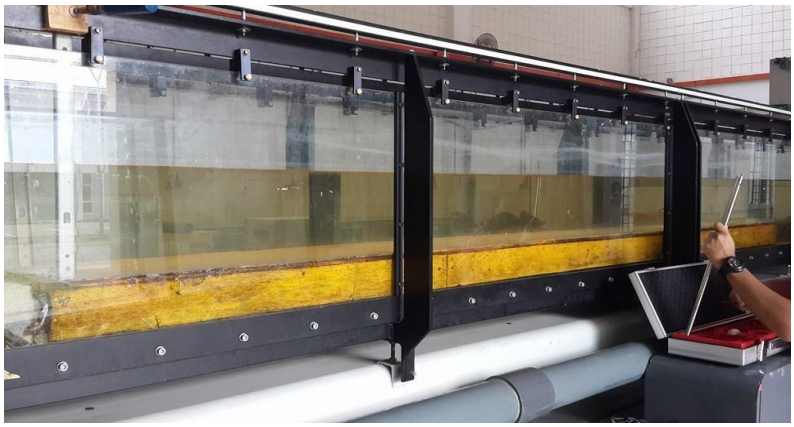

Figure 3-8*: False Floor*

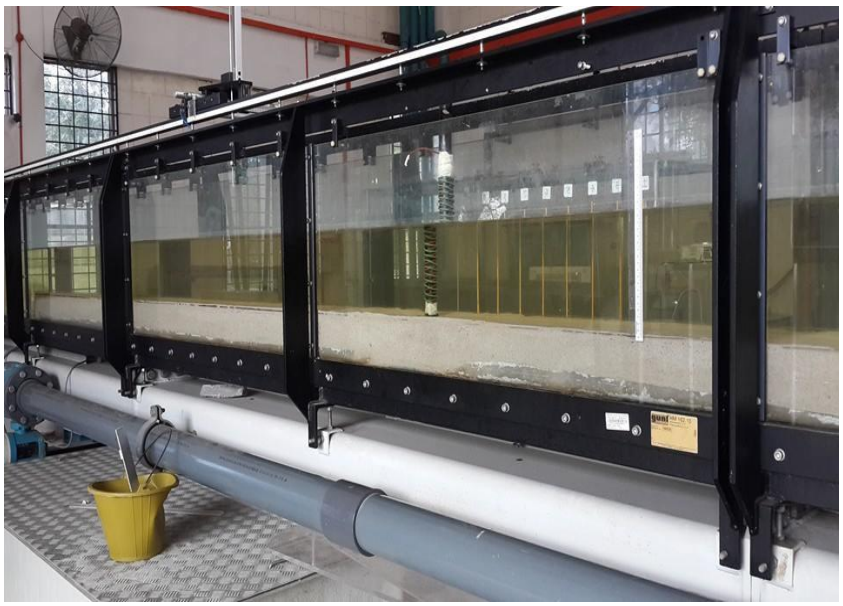

Figure 3-9*: Sand Filled Up In The Flume*

Figure 3-10: *Underlying Geo Textile On Bed Of Flume*

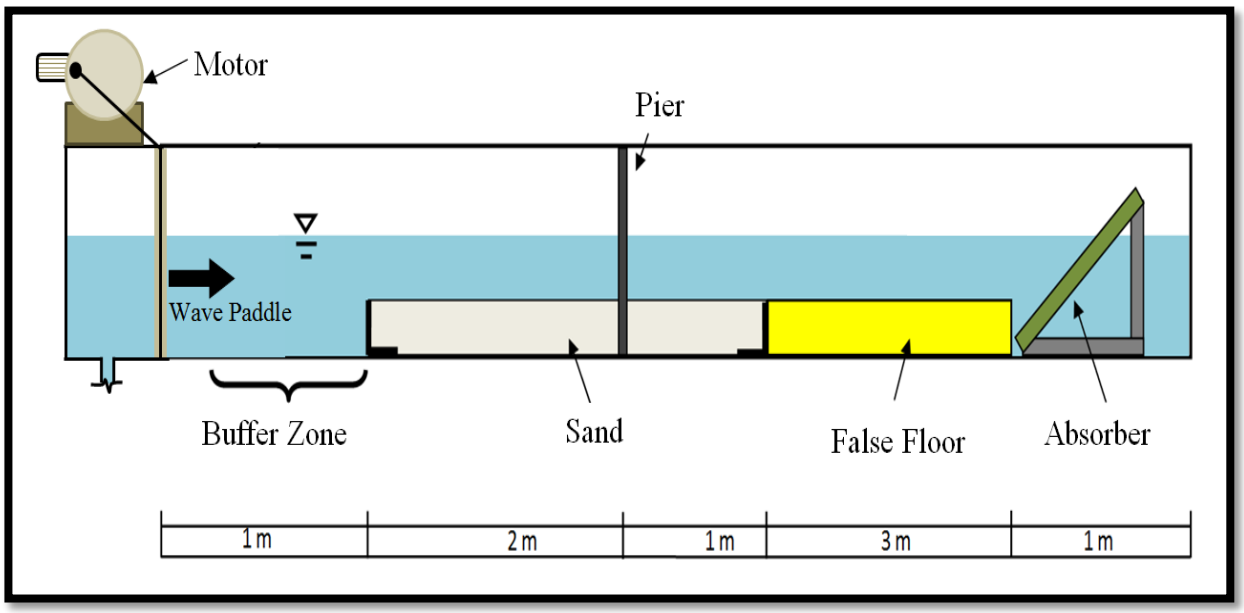

Figure 3-11*: Flume set up in the experiment*

3.6 Test Programme

Table 3-3: Matrix of the experiment.

Series of Test	Test Condition				Test I.D
Series A	Without Protection	Wave Period 1			A1
Series B	Single Cross-threaded	Wave Period 1	Cable Diameter= 2mm	Thread Angle= 15°	B1
			Cable Diameter= 2mm	Thread Angle= 30°	B2
			Cable Diameter= 3mm	Thread Angle= 15°	B3
			Cable Diameter= 3mm	Thread Angle= 30°	B4
Series C	Double Cross-threaded	Wave Period 1	Cable Diameter= 2mm	Thread Angle= 15°	C1
			Cable Diameter= 2mm	Thread Angle= 30°	C2
			Cable Diameter= 3mm	Thread Angle= 15°	C3
			Cable Diameter= 3mm	Thread Angle= 30°	C4

Table 3-3 shows the series of tests that were conducted in this research. Experiment of Series A on scour hole around single pier without protection was exposed to a 1s of wave period. Each experiment was run for 30 to 45 minutes until the scour process generated an equilibrium scour hole. The depth of scour hole and the area of scour region were measured. The depth of scour hole at the middle of model was measured. ***Figure 3-12*** shows the line measurement for scour pattern in this experiment.

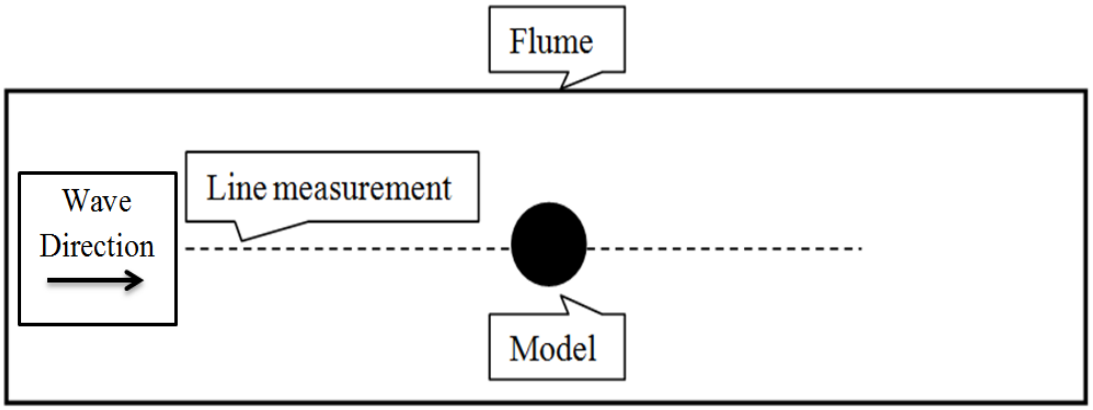

***Figure 3-12**: Line measurement for the experiment (Plan View).*

For Series B and C experiments of pier with protection were conducted. Each protected pier was exposed to the same wave period 1 in Series A test. This was done to evaluate the influence of cable diameter and thread angle on scour depth around of single and double cross-threaded pier. The scour depth and area from coverage resulted by the models were compared with the unprotected pier. Efficiency of scour reduction for each models are calculated as in ***Equation (3.1).***

$$Efficiency = \left(\frac{Eroded\ area\ of\ protected\ pier, a_2}{Eroded\ area\ of\ unprotected\ pier, A_2}\right) \times 100\% \qquad \textbf{(3.1)}$$

3.7 Kinematics and Dynamics

"Kinematics" generally refers to the study of properties of motion, position, velocity, acceleration, while "Dynamics" means a study of the rules governing the interactions of these particles. Hence, Kinematics and dynamics are significant mathematical gears to understand the fundamental features of the associated wave phenomena. ***Equations 3.2 - 3.9*** shows the wave parameters that has been calculated in this study.

a) Wave Celerity:

$$C = \frac{L}{T} = \frac{gT}{2\pi}\tanh\left(\frac{2\pi d}{L}\right) \qquad \textbf{(3.2)}$$

b) Water Particle Velocity:

$$u = \left(\frac{H}{2}\right)\left(\frac{gT}{L}\right)\left(\frac{cosh[2\pi(z+d)/L]}{cosh[2\pi d/L]}\right)\cos\theta \qquad \textbf{(3.3)}$$

$$w = \left(\frac{H}{2}\right)\left(\frac{gT}{L}\right)\left(\frac{sinh[2\pi(z+d)/L]}{cosh[2\pi d/L]}\right)\sin\theta \qquad \textbf{(3.4)}$$

c) Water Particle Accelerations:

$$\alpha_x = \left(\frac{g\pi H}{L}\right)\left(\frac{cosh[2\pi(z+d)/L]}{cosh[2\pi d/L]}\right)\sin\theta \quad \textbf{(3.5)}$$

$$\alpha_z = \left(\frac{g\pi H}{L}\right)\left(\frac{sinh[2\pi(z+d)/L]}{cosh[2\pi d/L]}\right)\cos\theta \quad \textbf{(3.6)}$$

d) Water particle Displacement:

$$\xi = \left(\frac{H}{2}\right)\left(\frac{cosh[2\pi(z+d)/L]}{sinh[2\pi d/L]}\right)\sin\theta \quad \textbf{(3.7)}$$

$$\zeta = \left(\frac{H}{2}\right)\left(\frac{sinh[2\pi(z+d)/L]}{sinh[2\pi d/L]}\right)\cos\theta \quad \textbf{(3.8)}$$

e) Subsurface Pressure:

$$p = (\rho g\eta)\left(\frac{cosh[2\pi(z+d)/L]}{cosh[2\pi d/L]}\right) - \rho g z \quad \textbf{(3.9)}$$

CHAPTER 4
EXPERIMANTAL RESULTS AND DISCUSSION

4.1 Introduction

This chapter presents the results obtained from the experiments of series A, B and C. The experiment of Series B and C was conducted where the result of scour formation and it pattern are observed and compared to unprotected pier. Results are presented according to each models type. Then, performance of the models in reducing scour depth is discussed also in this chapter.

4.2 Wave Kinematics

4.2.1 Wavelength

In this experiment the water depth, *d* was fixed at 20 cm and the wave period, *T* was maintained at 1s. To calculate the local wavelength, *L* it is first required to determine the deepwater wavelength, L_o by using ***equation (4.1).***

Therefore, the L_o for T = 1s is 1.56m.

$$L_0 = \frac{gT^2}{2\pi} \quad \textbf{(4.1)}$$

where g = gravitational acceleration (m/s^2).

d/L_o= 0.128, by referring to the wave table from Shore Protection Manual d/L = 0.1649 is obtained. Therefore the calculated wave length, *L* is 1.21 m. Wave classification is also done whereby the wave type used in this experiment is transitional water. Wave classification is made according to the magnitude of *d/L*, where it satisfies the properties $1/25<d/L<1/2$.

4.2.2 Wave Profile

A wave profile is obtained by a plot of displacement of water particle relative to the still water level for a period of time. Linear wave theory considers the wave form is sinusoidal and regular. The displacement of the sinusoidal water surface relative to the SWL (η) can be time mathematically expressed as:

$$\eta = \frac{H}{2}\cos\theta \qquad \textbf{(4.2)}$$

where *H* and θ are the incident wave height and phase angle respectively.

In this study, the test models were subjected to waves of 3cm throughout the experiment. The profile of the waves calculated from equation (4.2) is presented in ***Table 4***-1 and is graphically given in ***Figure 4-1***.

Table 4-1*: Determination of Wave Profile Table*

Degree, θ	Rads, θ	Cos θ	η=H/2 Cos θ
-90	-π/2	0	0.000
0	0	1	0.030
90	π/2	0	0.000
180	π	-1	-0.030
270	3π/2	0	0.000
360	2π	1	0.030
450	5π/2	0	0.000
540	3π	-1	-0.030
630	7π/2	0	0.000
720	4π	1	0.030
810	9π/2	0	0.000

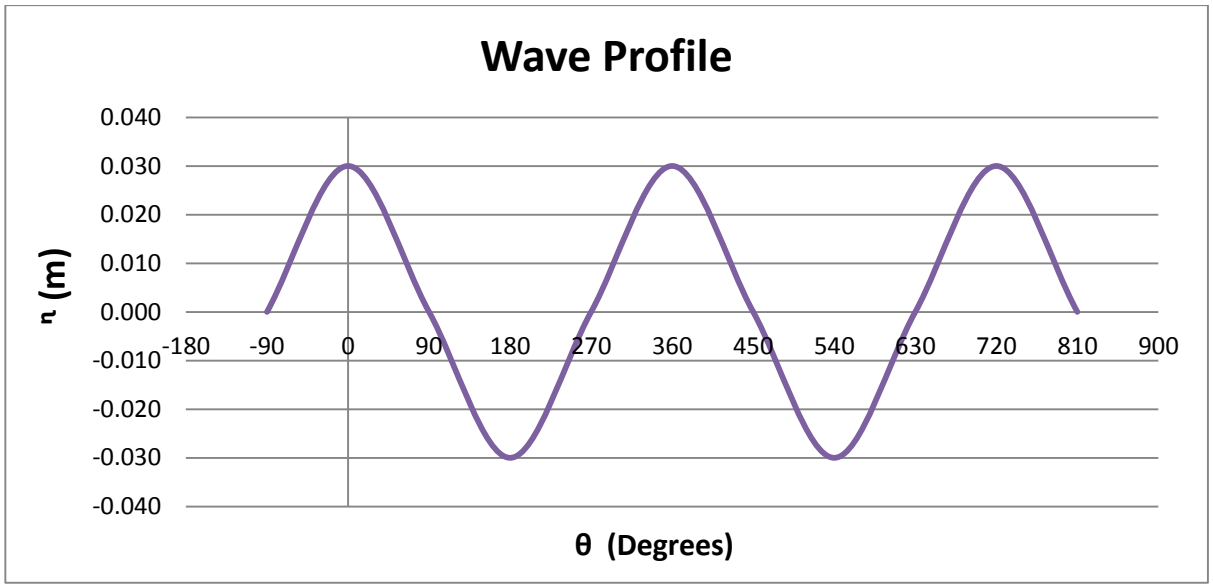

***Figure 4-1**: Wave Profile*

4.2.3 Kinematics and Dynamics

The kinematics and dynamic properties of the water particles of H=0.03m and T=1s for different depths below the still water level computed using the ***equation (3.2) to (3.9)***, are presented in ***Table 4-2***. To give a better understanding of the hydrodynamics of the water particles, the data in ***Table 4-2*** were translated into a form of graphical presentation as shown in ***Figure 4-2*** *to* ***Figure 4-8.***

Figure 4-2 and **Figure 4-3** display the horizontal and vertical water particle velocities, respectively. It is seen from the figure that the horizontal water particle velocity reduces exponentially as water depth increases. At free surface, the horizontal velocity is being the maximum (u = 0.246 m/s). On another hand, the horizontal velocity of water particle becomes minimal as it approaches to the bottom (u = 0.155 m/s). For vertical water particle velocity, the reduction of velocity, *w* with the increase of water depth follows a weak exponential trend. The vertical water particle velocity, $\underline{w}$ were computed as 0.191 m/s and 0 m/s at free surface and sea bottom, respectively.

***Table 4-2**: Wave Parameters with corresponding Depth*

Z(m)	Velocity (m/s)		Acceleration (m/s^2)		Displacement (m)		Pressure (N/m)
	Horizontal, u	Vertical, w	Horizontal, α_x	Vertical, α_z	Horizontal, ξ	Vertical, ζ	
0.000	0.246	0.191	1.547	-1.203	-0.036	0.028	305.403
-0.020	0.228	0.167	1.430	-1.048	-0.033	0.024	483.389
-0.040	0.212	0.144	1.329	-0.905	-0.031	0.021	664.424
-0.060	0.198	0.123	1.242	-0.772	-0.029	0.018	848.290
-0.080	0.186	0.103	1.169	-0.647	-0.027	0.015	1034.803
-0.100	0.176	0.084	1.108	-0.528	-0.026	0.012	1223.807
-0.120	0.168	0.066	1.059	-0.416	-0.024	0.010	1415.170
-0.140	0.162	0.049	1.021	-0.308	-0.024	0.007	1608.789
-0.160	0.158	0.032	0.994	-0.204	-0.023	0.005	1804.584
-0.180	0.156	0.016	0.979	-0.101	-0.023	0.002	2002.498
-0.200	0.155	0.000	0.973	0.000	-0.022	0.000	2202.497

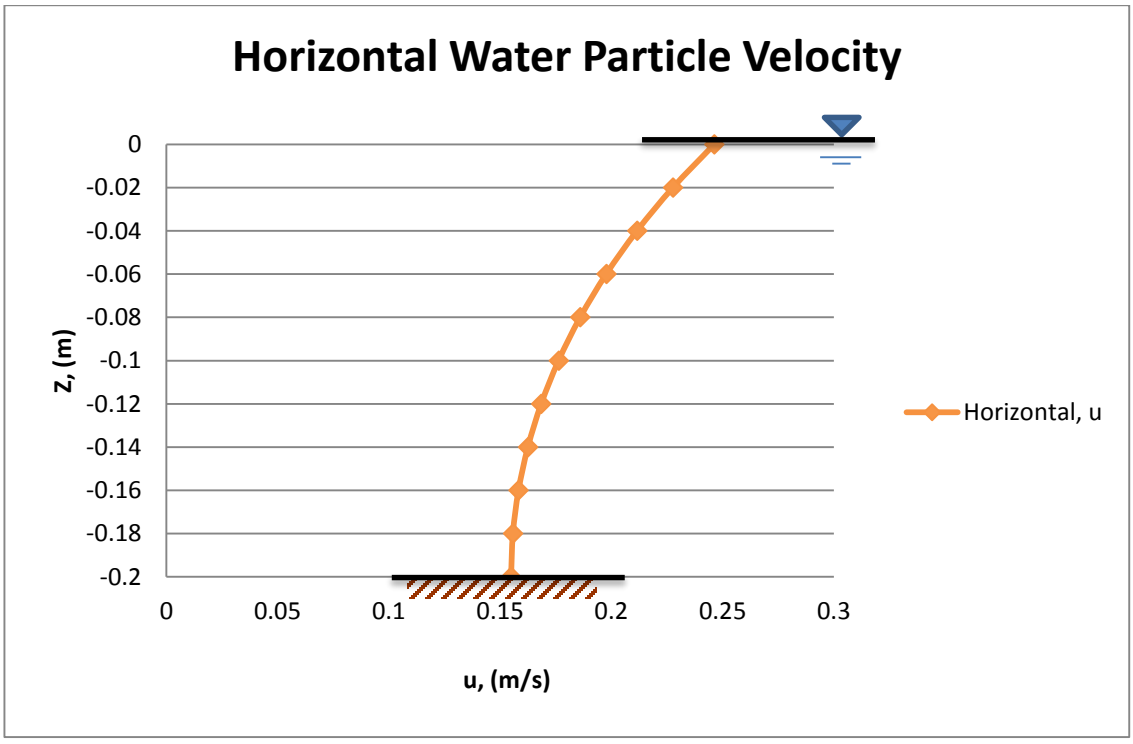

***Figure 4-2**: Horizontal Water Particle Velocity*

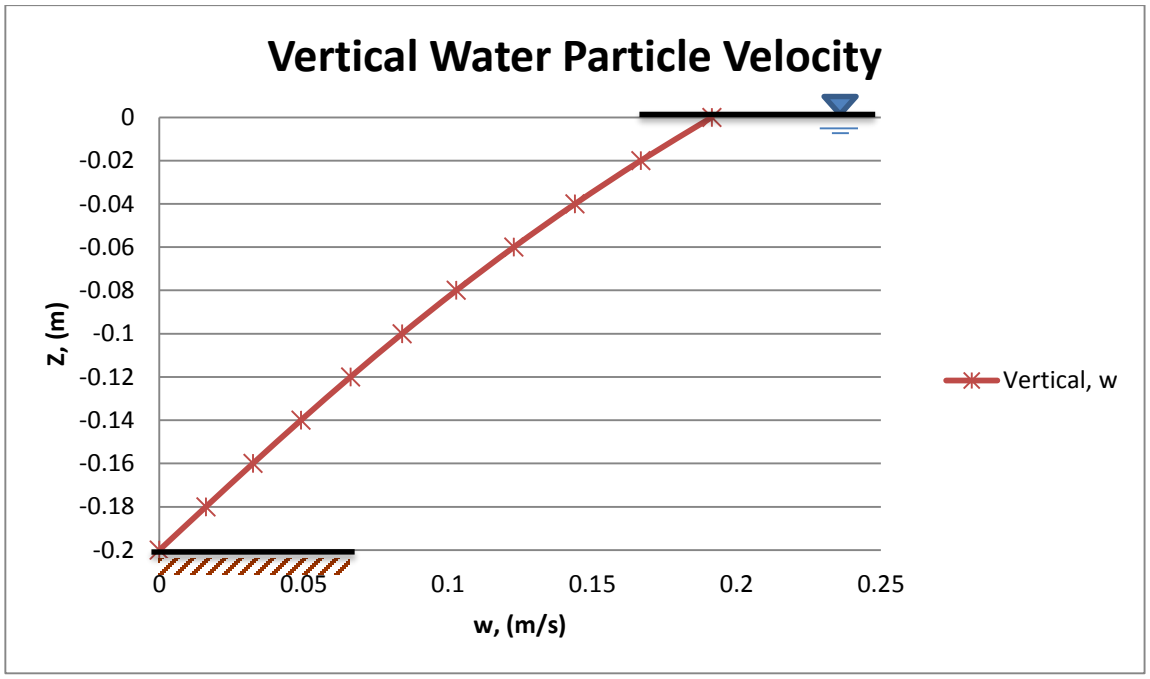

***Figure 4-3**: Vertical Water Particle Velocity*

Figure 4-4 and ***Figure 4-5*** exhibits the horizontal and vertical water particle acceleration. It is observed that the horizontal water particle acceleration, α_x decreases exponentially with increasing of depth. The horizontal water particle acceleration, αx at the free surface and bottom are 1.547 m/s^2 and 0.973 m/s^2 respectively.

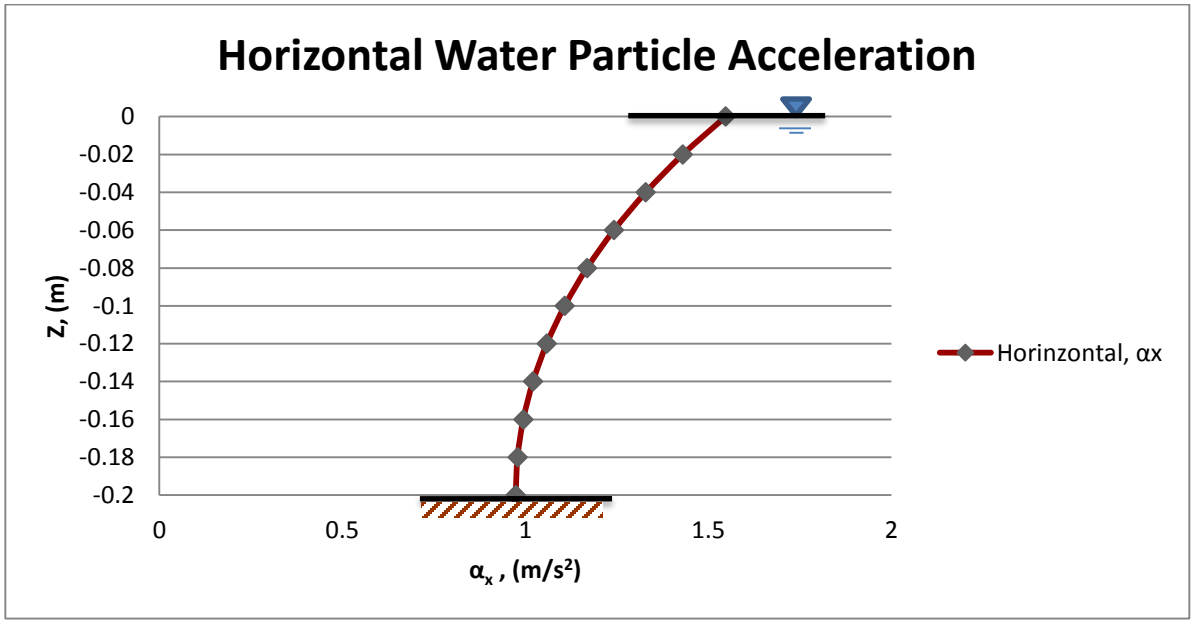

***Figure 4-4**: Horizontal Water Particle Acceleration*

Meanwhile ***Figure 4-5*** illustrates that the vertical water acceleration, α_z increases as the depth increases. The vertical water velocity, α_z at free surface is -1.203 m/s^2 and zero at the bottom. From the outcome, it shows that horizontal and vertical water particle acceleration has opposing trend.

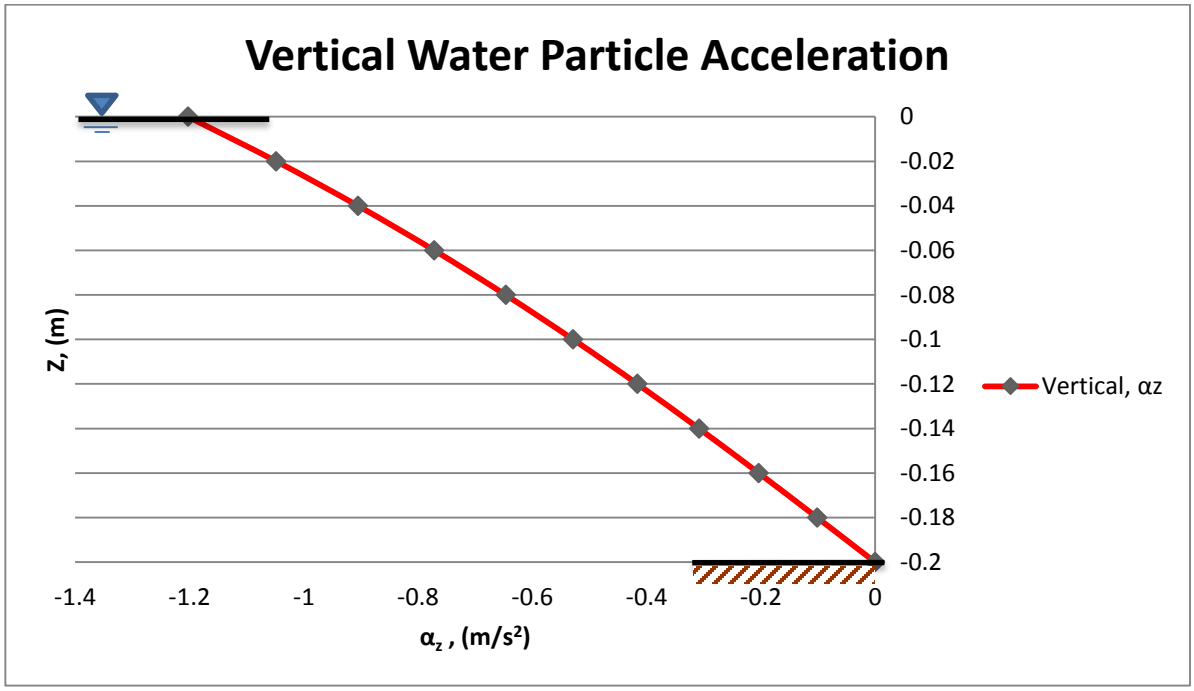

Figure 4-5*: Vertical Water Particle Acceleration*

The horizontal water particle displacement is demonstrated in ***Figure 4-6***. It is obvious that the horizontal water particle displacement, ξ increases exponentially with the increasing depth. The horizontal water particle displacement, ξ at free surface and bottom are -0.036 and -0.023 m, respectively.

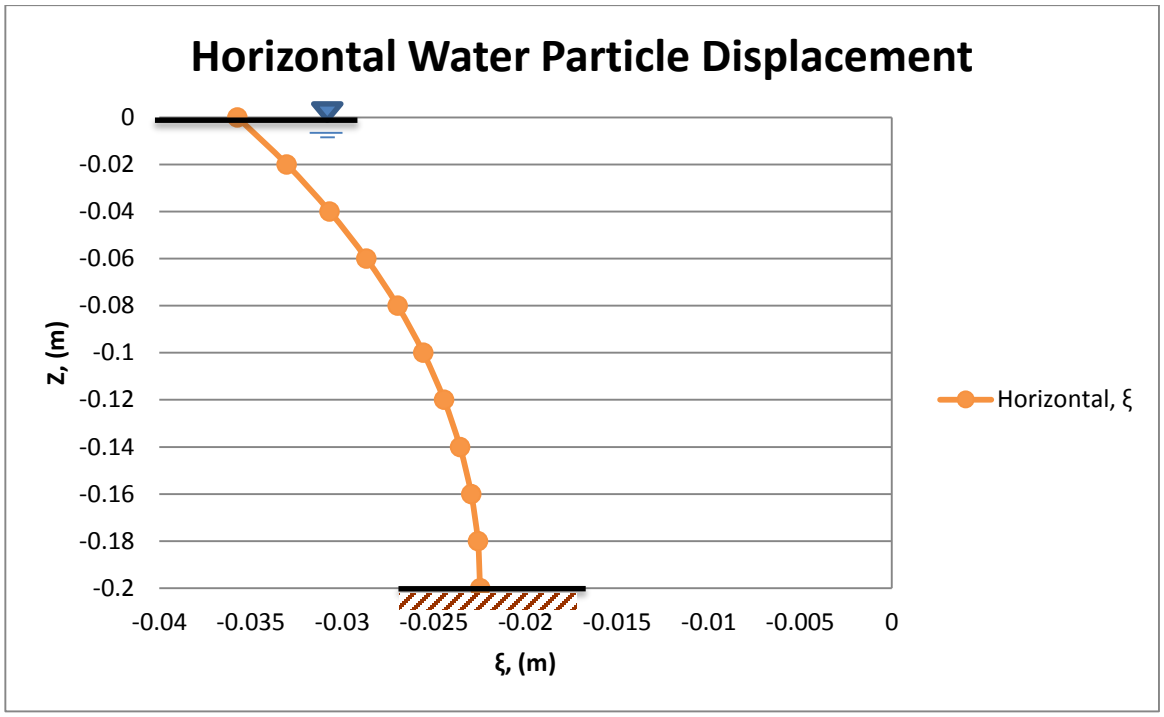

***Figure 4-6**: Horizontal Water Particle Displacement*

For vertical water particle displacement as shown in ***Figure 4-7***, it is observed that the vertical water particle displacement, ζ reduces exponentially with an increase of water depth, which is almost directly proportional as the water depth decreases. The vertical water particle displacement, ζ at free surface and bottom are 0.028 and 0 m, respectively. From the findings it portraits the elliptical shape of water particle with smaller horizontal displacement at free surface. At the sea bottom the water particle moves in horizontal and reversing trend.

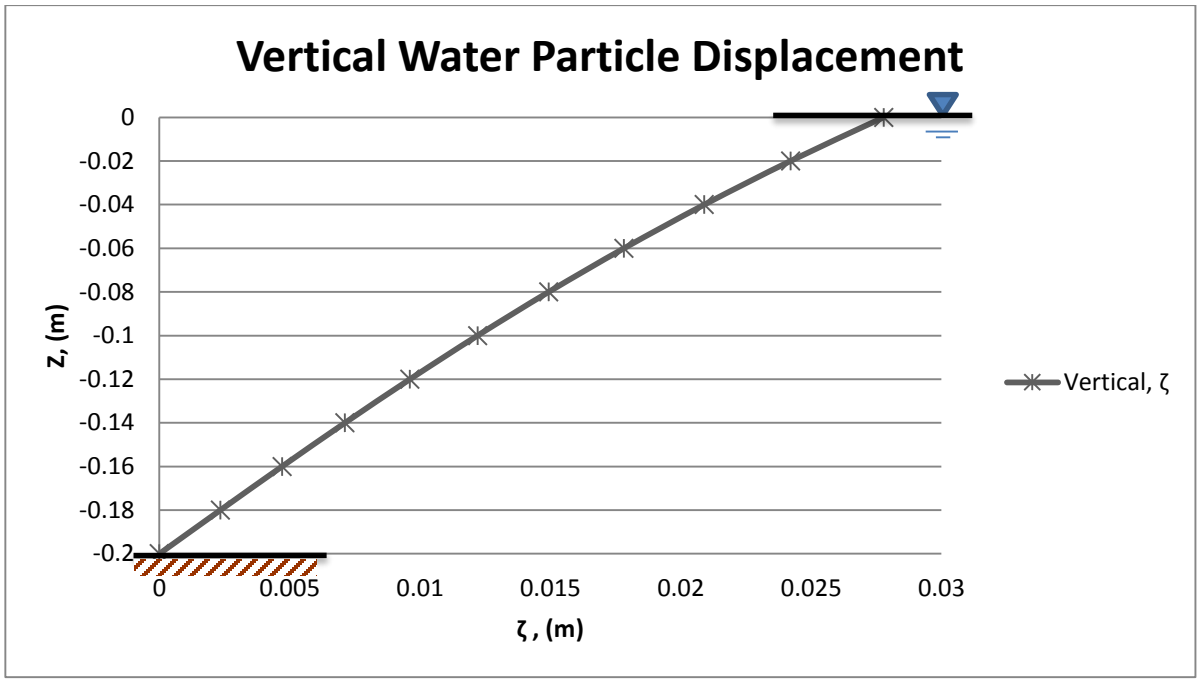

Figure 4-7: *Vertical Water Particle Displacement*

The dynamic properties of the wave of H = 0.03m and T = 1s were explored in the form of subsurface pressure along the water column, as shown in ***Figure 4-8.*** It is found that the pressure at the free surface is zero and increases linearly as water depth increases. At the bottom the pressure reaches the maximum value 2202 N/m.

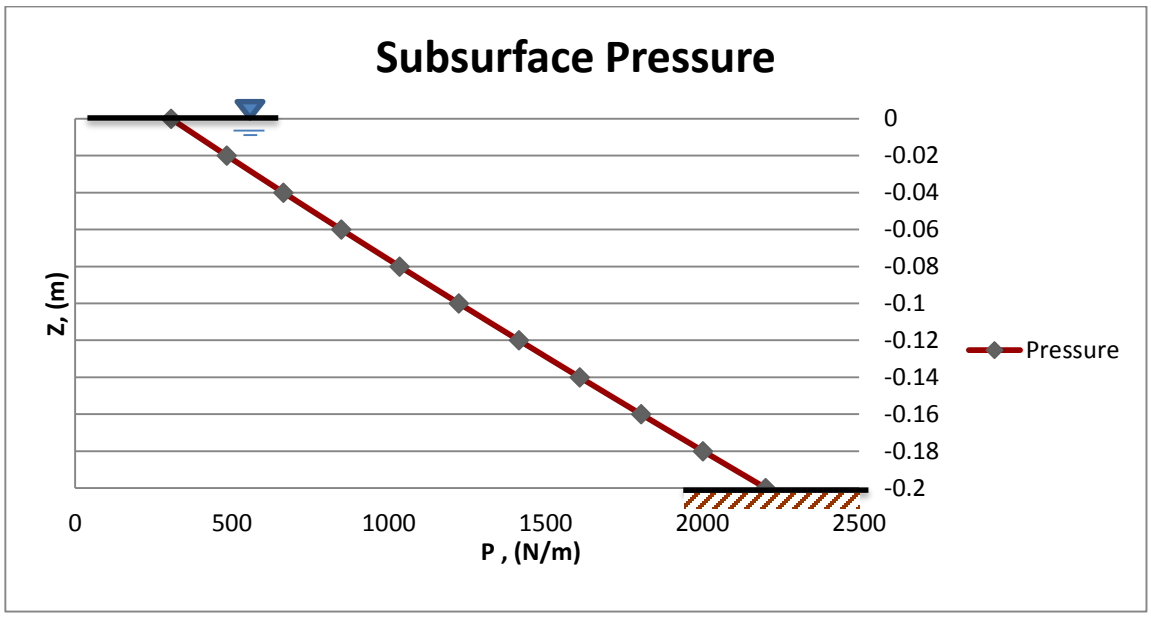

Figure 4-8*: Subsurface Pressure*

It is important to emphaze the water particle properties at the bottom as the hydrodynamic will govern the sedimentary movement in the vicinity of the test models. Under regular wave condition, the bottom is subjected to a horizontal displacement of 2.25 cm from the mean position (with no vertical water particle displacement) at a velocity of 0.15 m/s. In another hand, the horizontal water particles interact with the bottom sediment for a maximum length of 45 cm under a complete wave cycle.

4.3 Unprotected pier

A series of experiments were conducted to study the scour formation develop in the vicinity of the test models. ***Figure 4-9*** shows the sedimentary profile measured along the centreline of the unprotected pier. It is found that the amount of erosion is more than that of accretion (deposition) in both upstream and downstream of the unprotected pier. From ***Table 4-3*** it is shown that the effected distances are approximately 15cm to the pier and 31 cm from the pier. The largest scour depth measured is 0.8 cm at the front and 1.1 cm at the lee. Scour erosion at the front is mainly due to the horseshoe vortex which continues to dig the bed. Sediments are transported downstream, and eventually settle in regions of lower turbulence.

***Table 4-3**: Unprotected Pier Test Result*

Test I.D	Pier Diameter, D (mm)	Measured Scour Length, L Upstream (cm)	Measured Scour Length, L Downstream(cm)	Measured Upstream Max. Scour Depth, $y_{1,u}$ (cm)	Up-stream eroded area,A 2 (cm^2)	Measured Down-stream Max. Scour Depth, y2,u (cm)	Down-stream eroded. B2 area, (cm^2)
A1	30	15.5	31.5	0.8	4.2	1.1	7.55

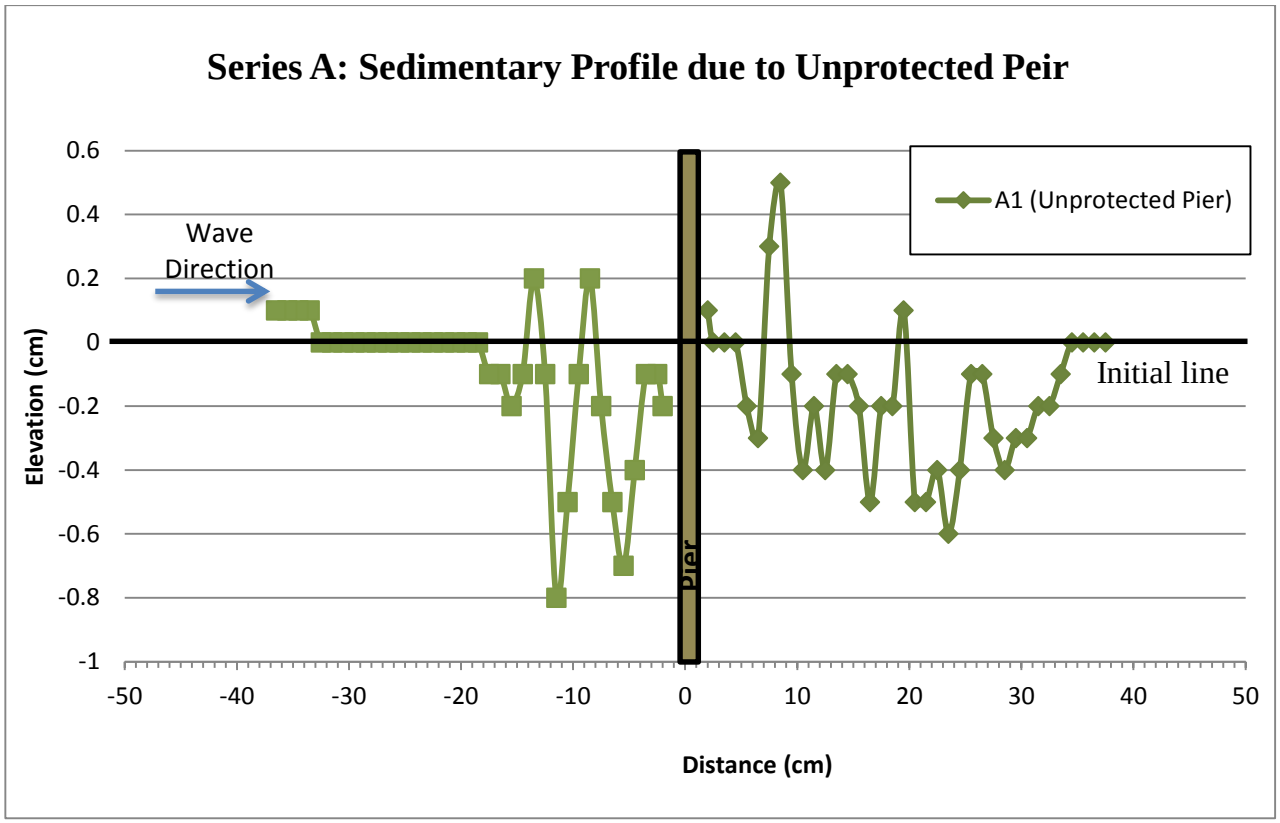

***Figure 4-9**: Alteration of Sediment Profile due to Unprotected Pier*

4.4 Single cross-threaded pier

Figure 4-10 and ***Figure 4-11*** shows the bottom profile in the vicinity of the piers of b/D=0.067 for θ= 15^0 and 30^0 at 45 minutes after the experiment, respectively. It is found that the bottom profile alters significantly after 45 minutes of the experiment sediment deposit and erodes are presented by the plotted points above and below the initial level (datum). Significant erosion is found right at the front of the piers followed by deposition at the distance from the piers. At the lee of the piers, the alteration of bottom profile is subjected to the thread angle, θ. For instance the pier of θ= 15^0 triggers significant of sedimentation; whereas, an appreciable of erosion happens at the toe of the pier of θ= 30^0. The maximum scour depth recorded by piers with θ= 15^0 and 30^0 are 0.7cm and 0.9cm at the downstream, respectively. From the above observation, it can be deduced that the pier of b/D=0.067 for θ= 15^0 is more suitable to be adapted as a supporting structure.

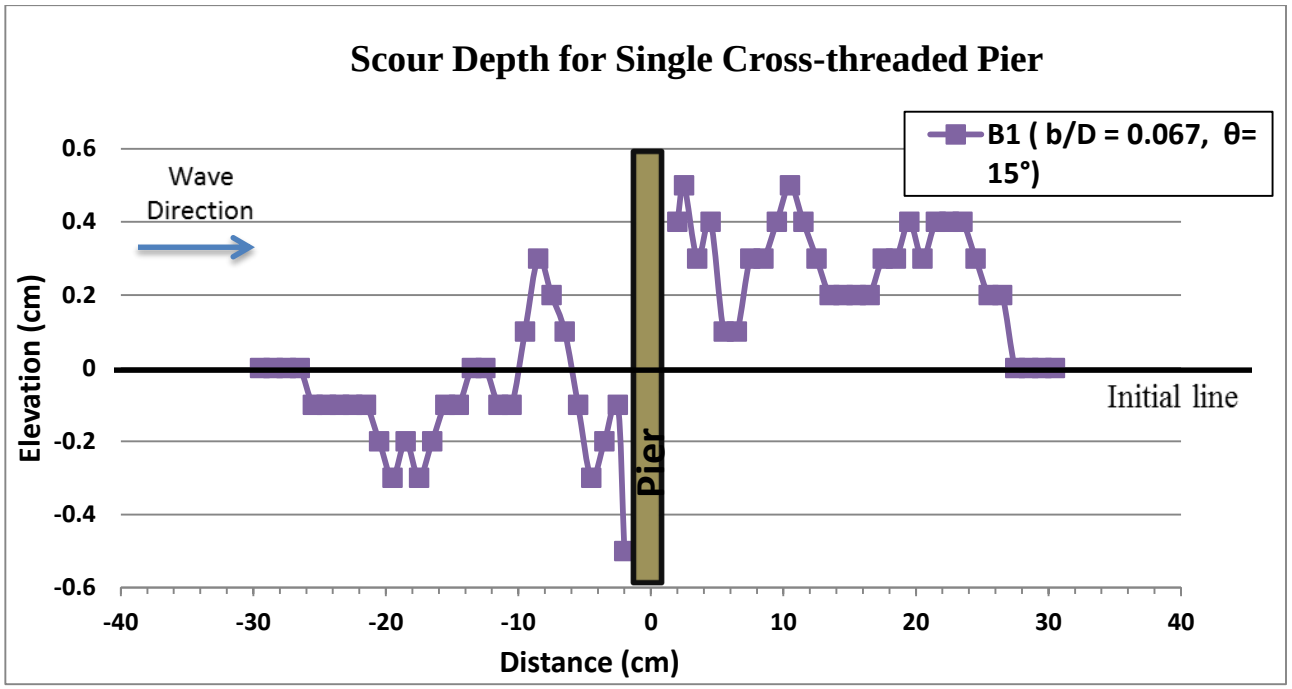

***Figure 4-10**: Scour Depth for Single Cross-Threaded Pier (B1, b/d = 0.067, θ = 15°)*

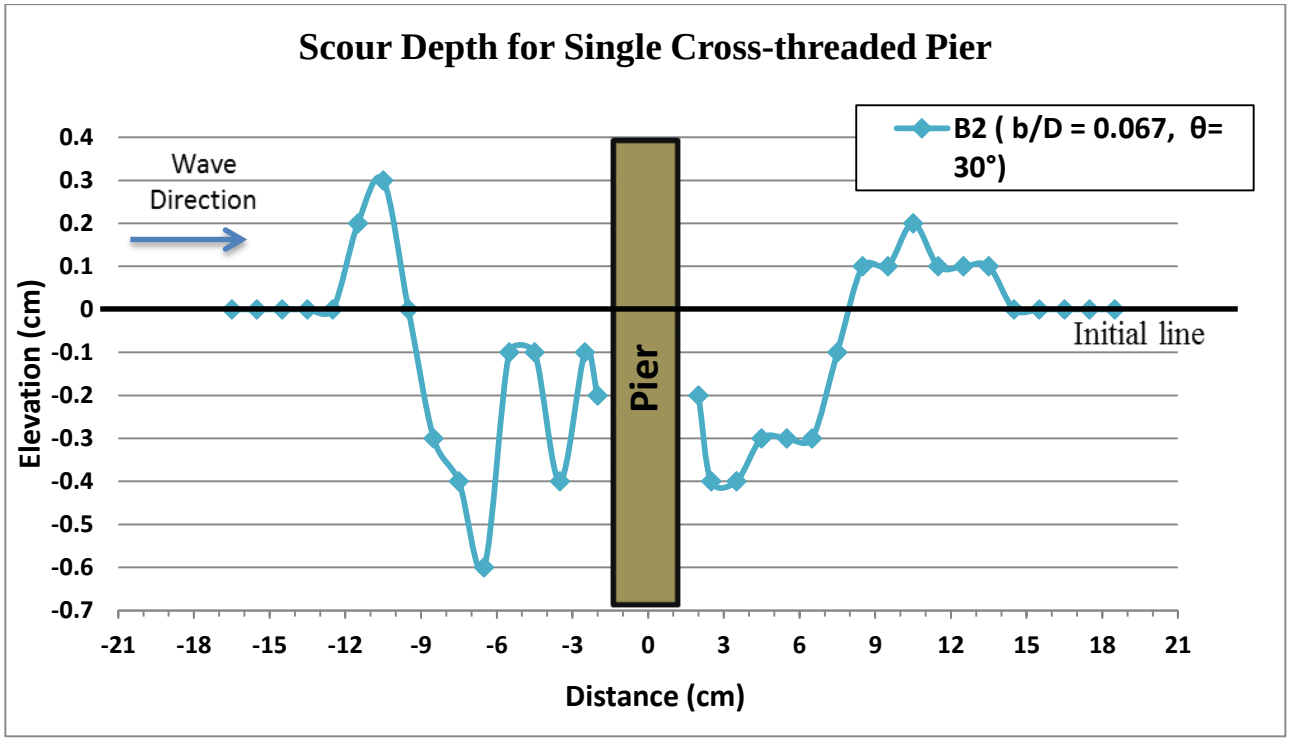

***Figure 4-11**: Scour Depth for Single Cross-Threaded Pier (B2, b/d = 0.067, θ = 30°)*

Figure 4-12 and ***Figure 4-13*** present the bottom profiles of b/D=0.1 for θ= 15^0 and 30^0, respectively. Considerable erosion is observed in the vicinity of the pier of θ= 30^0. A maximum scour depth of approximately 0.8cm developed at the front of the pier. In comparison with the pier of θ= 15^0, the amount of erosion happened at the front of the pile is relatively small and may not impose appreciable impact to the structure. However, the erosion formed behind the pier is regarded to be significant.

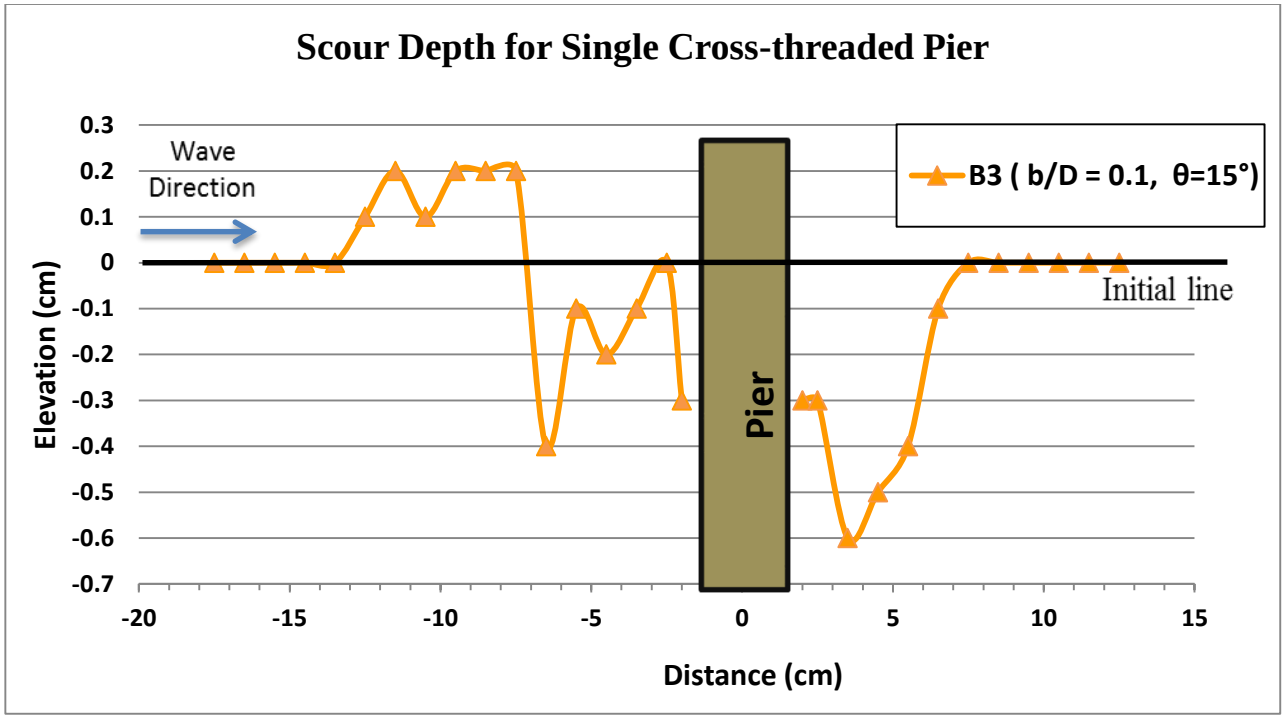

Figure 4-12: *Scour Depth for Single Cross-Threaded Pier (B3, b/d = 0.1, θ = 15°)*

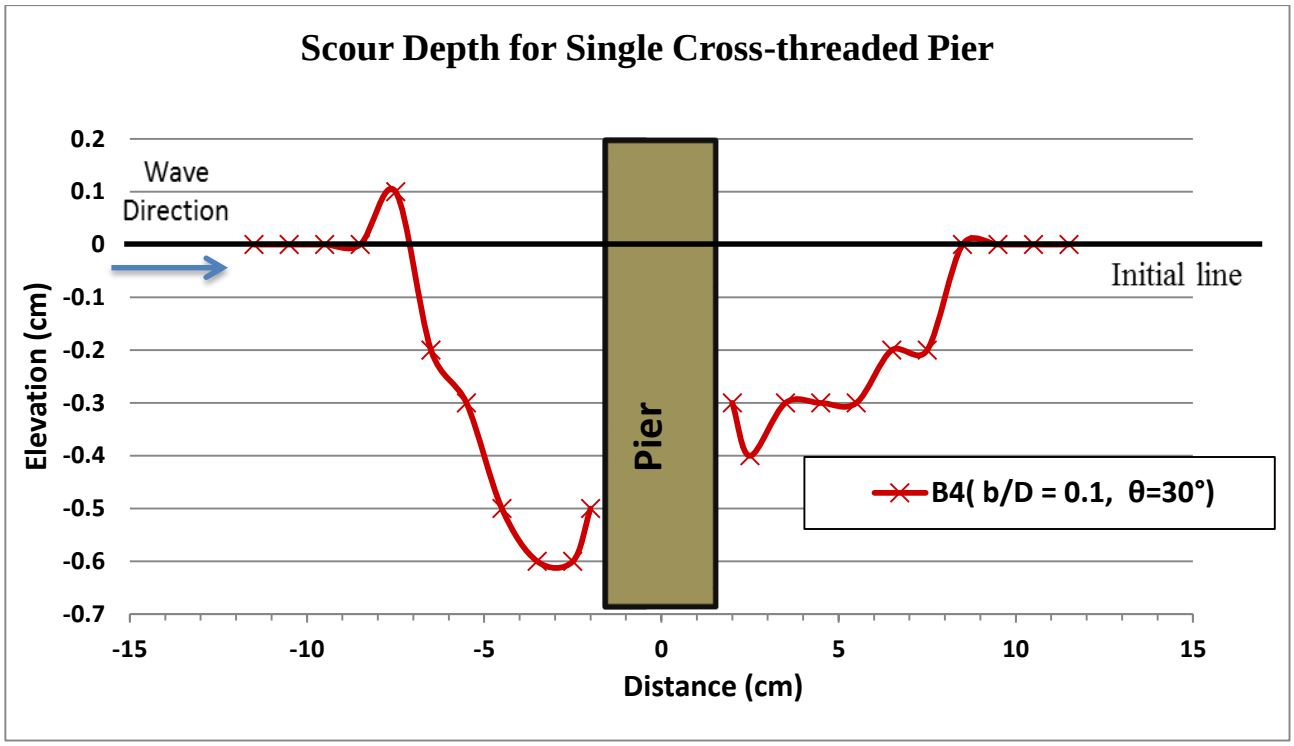

***Figure 4-13**: Scour Depth for Single Cross-Threaded Pier (B4, b/d = 0.1, θ = 30°)*

Figure 4-14 compares the bottom profiles of the unprotected piers and the protected piers with different b/D and θ. Overall it can be qualitatively judge that the protected piers do help to minimize the scour depth in their area proximately. The summarized results are shown in ***Table 4-4***. Based on the table it is recorded that b/D=0.067 for θ= 15^0 has the longest scour length at the upstream and downstream and b/D=0.1 for θ= 30^0 has the shortest length of scouring at both sides approximately 5.5 cm. In conclusion, the upstream scour due to the piers of single cross thread is affected by the relative thread width and its angle.

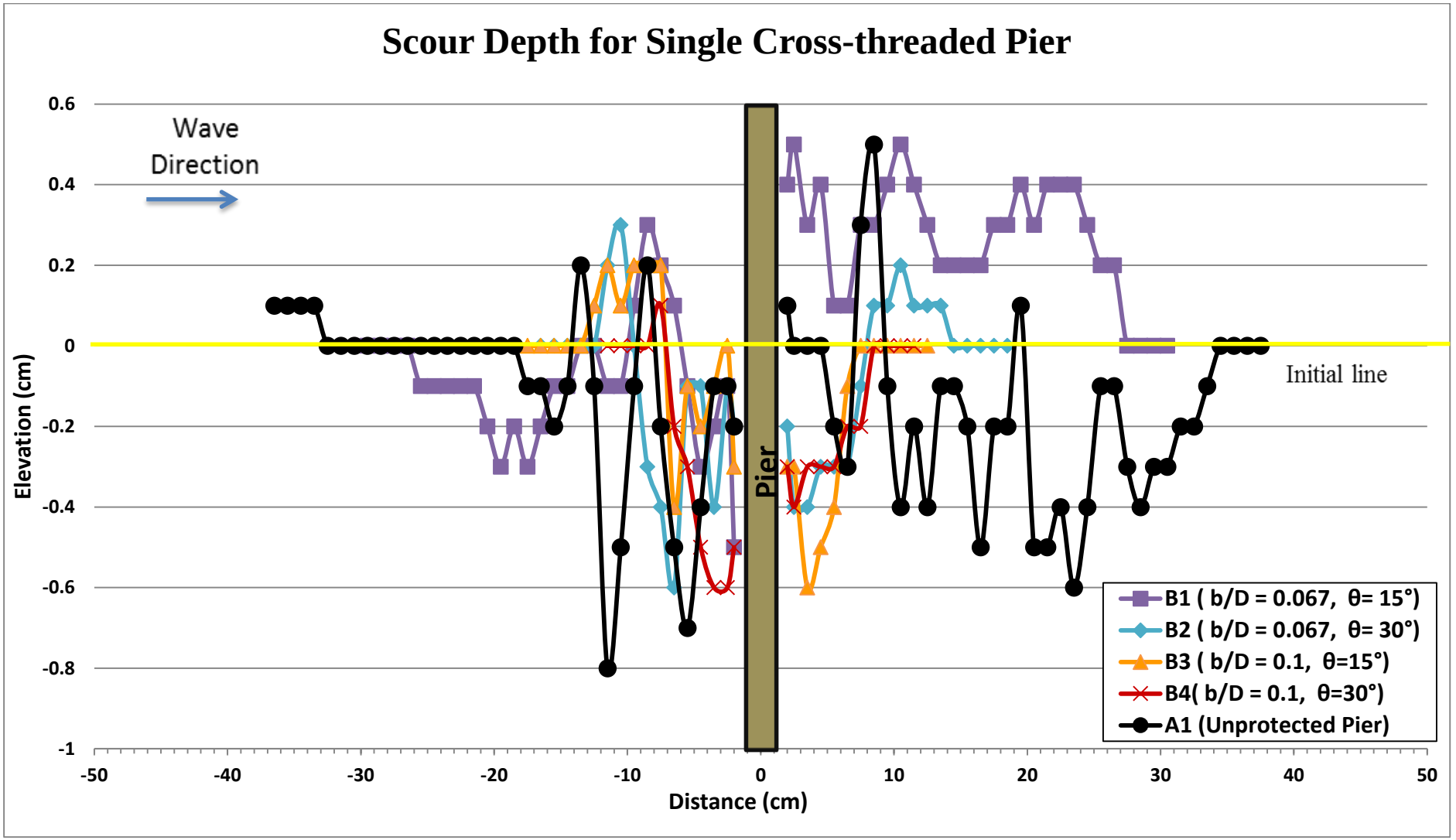

***Figure 4-14**: Scour Depth for Single Cross-Threaded Pier*

Table 4-4: Single Cross-Threaded Pier Test Results

Test I.D	Cable Diameter, b (mm)	Thread Angle, θ (°)	b/D	Measured Scour Length, L Upstream (cm)	Measured Scour Length, L Downstream (cm)	Measured Upstream Max. Scour Depth, $y_{1,s}$ (cm)	Measured Downstream Max. Scour Depth, y2,s (cm)
B1	2	15	0.067	23.5	24.5	0.5	0.70
B2	2	30	0.067	9.5	11.5	0.4	0.90
B3	3	15	0.100	10.5	4.5	0.4	0.70
B4	3	30	0.100	5.5	5.5	0.8	0.40

4.5 Double cross-thread pier

For double cross-threaded piers of b/D=0.067as shown in ***Figure 4-15*** and ***Figure 4-15***, it is found that the one with $\theta = 30^0$ is subjected to severe erosion at its front compared to that of $\theta = 15^0$. At the lee of the piers a small undulation of profile is observed for both piers, with the maximum deposition and scour depths are 0.3 and 0.2 cm respectively. From the presented results, it can be said that the pier of $\theta = 15^0$ has better performance than of $\theta = 30^0$ in reducing the scour problem triggered by the supporting piers.

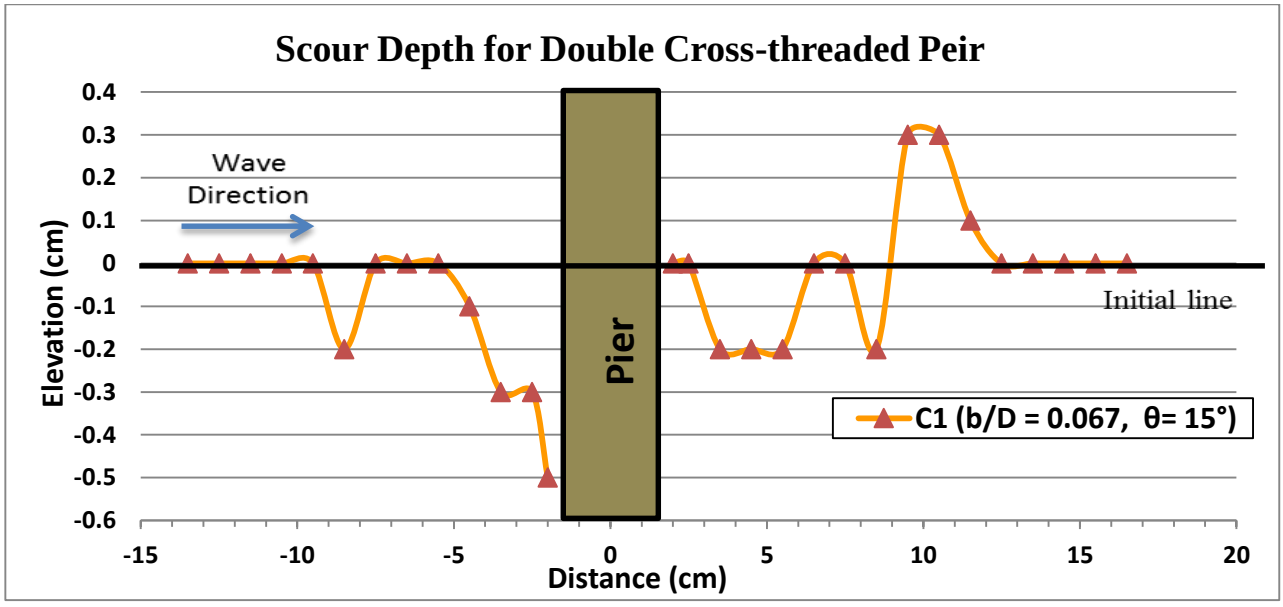

Figure 4-15: Scour Depth for Double Cross-Thread Pier (C1, b/d = 0.067, θ = 15°)

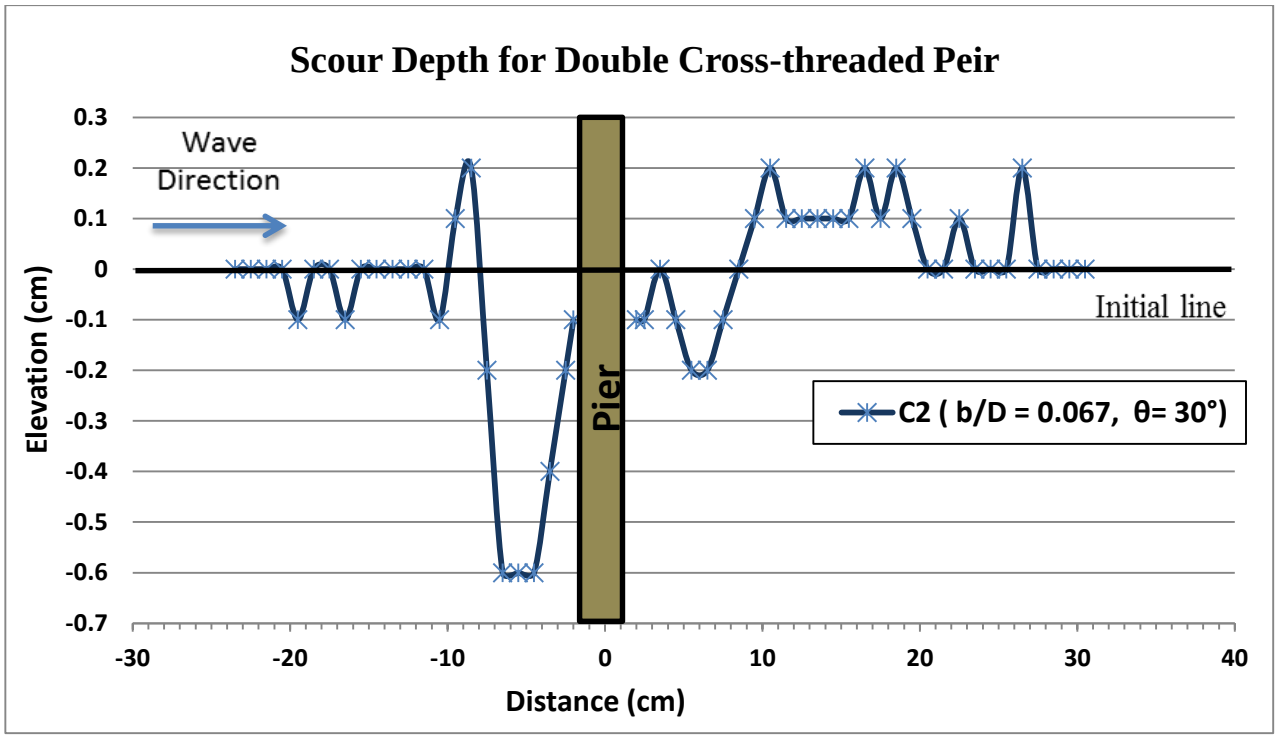

***Figure 4-16**: Scour Depth for Double Cross-Thread Pier (C2, b/d = 0.067, θ = 30º)*

As b/D increases from 0.067 to 0.100, it is also observed that the amount of local erosion is more obvious for the double cross-threaded pier of θ= 300 as shown in ***Figure 4-17 and Figure 4-18***. The amount of the maximum upstream and downstream scour depth of the double cross-threaded pile are presented in ***Table 4-5.***

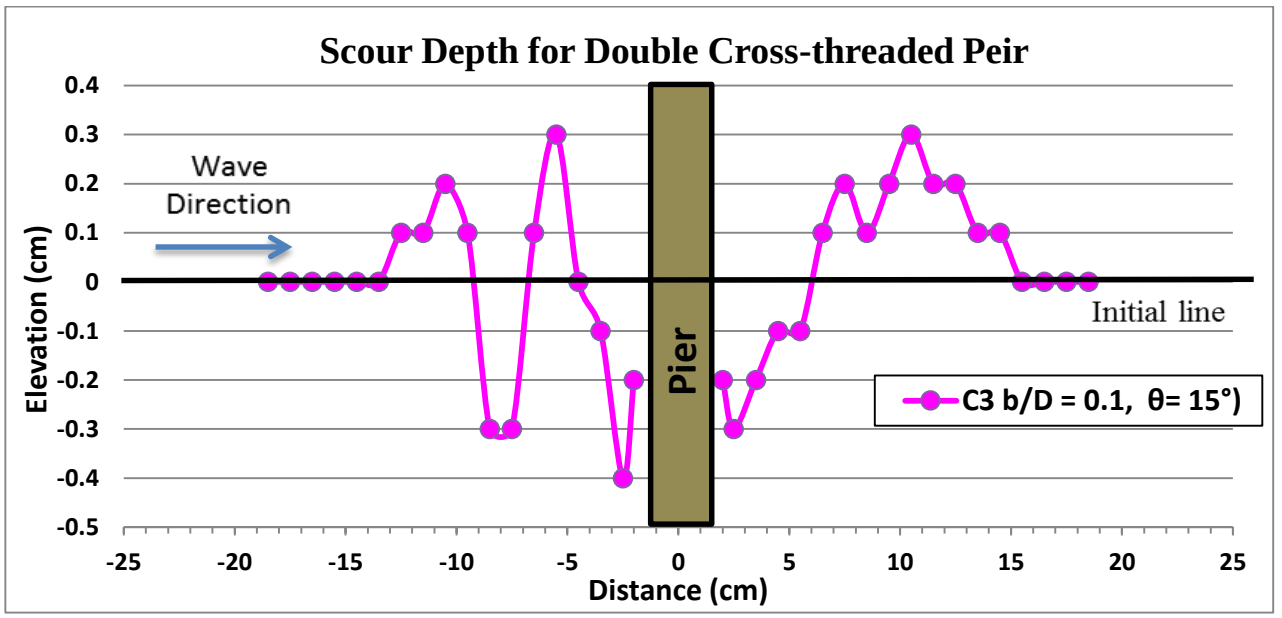

***Figure 4-17**: Scour Depth for Double Cross-Thread Pier (C3, b/d = 0.1, θ = 15º)*

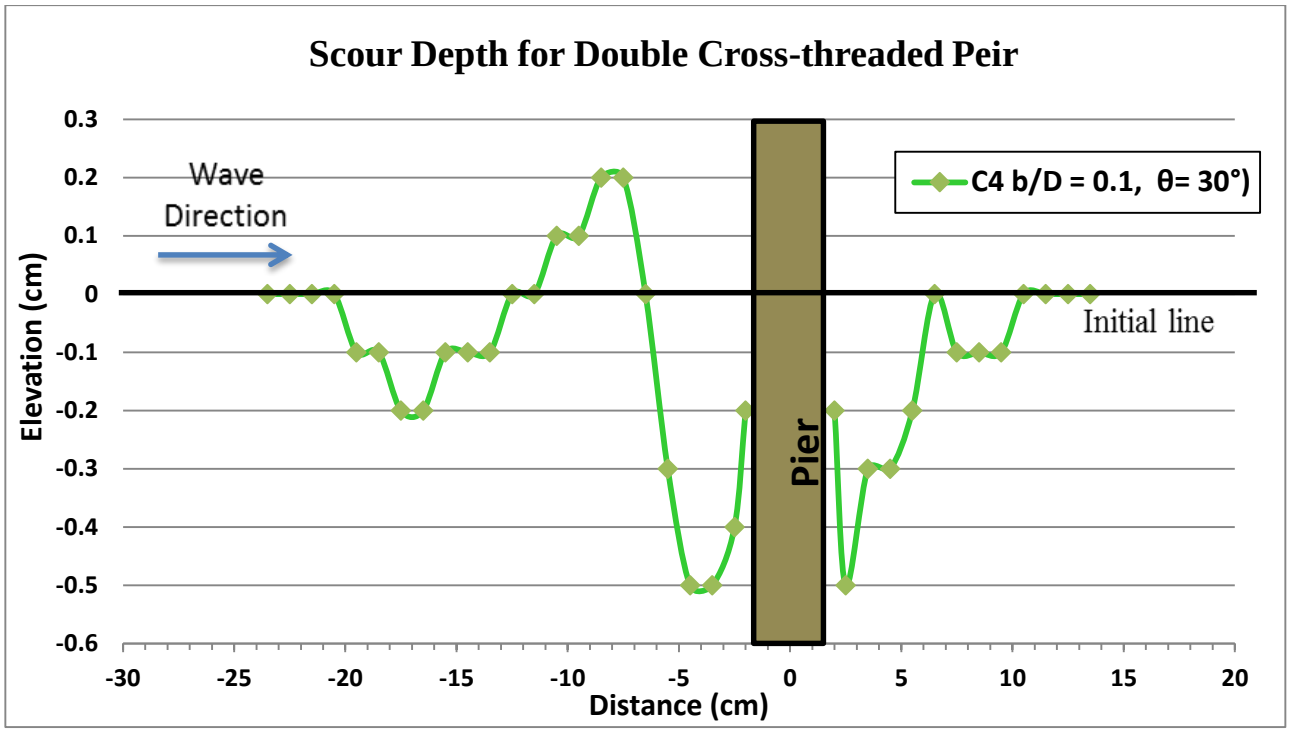

***Figure 4-18**: Scour Depth for Double Cross-Thread Pier (C4, b/d = 0.1, θ = 30º)*

For the double cross-threaded pier, comparison of the resulting bottom profiles due to piers of b/D= 0.067 and 0.1 and θ = 15º and θ = 30º are demonstrated in ***Figure 4-19***. It is clear from the figure that the double cross-threaded piers do help in reducing the scour problem at piers. ***Table 4-5*** shows the summarized results of double cross-threaded piers where it is observed that ,b/d = 0.067, θ = 30º has the longest scour length compared to other test series at both downstream and upstream respectively. The upstream scour due to the piers of double cross thread is affected by the relative thread width and its angle.

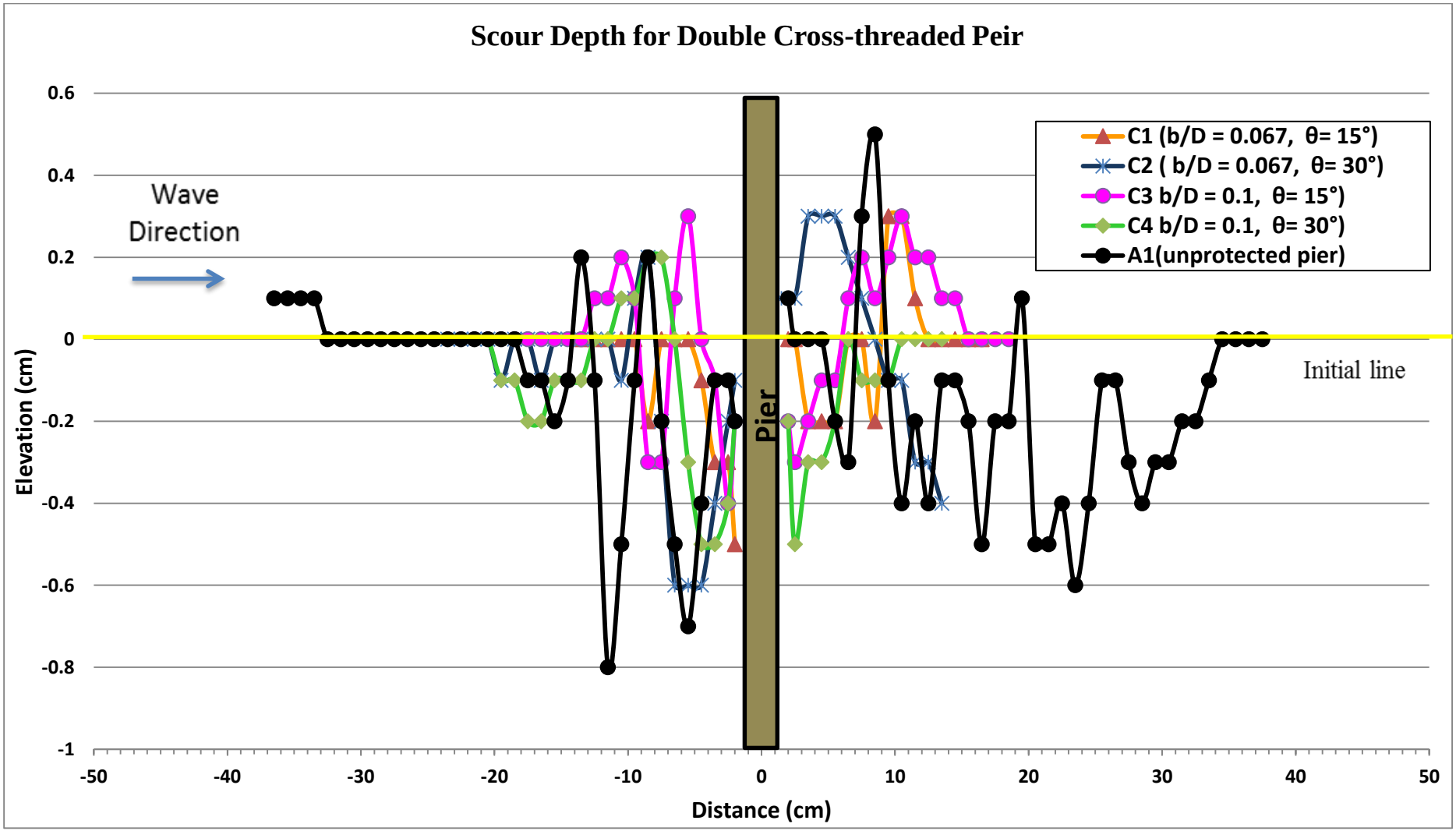

***Figure 4-19**: Scour Depth for Double Cross-Thread Pier*

Table 4-5: Double Cross-Thread Pier Test Results

Test I.D	Cable Diameter, b (mm)	Thread Angle, θ (°)	b/D	Measured Scour Length, L Upstream (cm)	Measured Scour Length, L Downstream (cm)	Measured Upstream Max. Scour depth, $y_{1,d}$ (cm)	Measured Downstream Max. Scour Depth, y2,d (cm)
C1	2	15	0.067	6.5	9.5	0.8	0.80
C2	2	30	0.067	17.5	17.5	0.6	0.80
C3	3	15	0.100	10.5	12.5	0.4	1.00
C4	3	30	0.100	17.5	7.5	0.5	0.80

4.6 Performance of Models

The eroded area of each test models are compared to unprotected pier eroded area to acquire efficiency. ***Table 4-6*** shows the summary result of scour reduction for all models of single cross-threaded pier and double cross-threaded pier. It is observed that the eroded area is greater in the used of double cross-threaded pile where 2.7cm^2 for b/D= 0.067 and θ = 30^o at the upstream region whereas, in the downstream zone the eroded area is utmost approximately 2.95cm^2 for b/D= 0.100 and θ = 30^o. It is also spotted that there is no eroded area for test model b/D= 0.067 and θ = 15^o. In general, the cross-threaded piers help to reduce the upstream scour at varying rates.

Table 4-6: Summary of the Scour Reduction Results.

Model type	Test I.D	Cable Diameter, b (mm)	Thread Angle, θ (°)	b/D	Up-stream eroded area, a2 (cm^2)	Up-stream Eroded Efficiency, (a2/A2)x 100%	Down-stream eroded area, b2 (cm^2)	Down-stream Eroded Efficiency, (b2/B2)x 100%
Single Cross-thread	B1	2	15	0.067	2.4	57%	0.00	100%
	B2	2	30	0.067	2.1	50%	1.80	24%
	B3	3	15	0.100	0.78	19%	1.80	24%
	B4	3	30	0.100	1.95	46%	1.45	19%
Double Cross-thread	C1	2	15	0.067	0.85	20%	0.95	13%
	C2	2	30	0.067	2.7	64%	0.55	7%
	C3	3	15	0.100	0.99	24%	0.68	9%
	C4	3	30	0.100	1.98	47%	2.95	39%

The comparison of efficiency of single cross-threaded pier and double cross-threaded pier for upstream and downstream are demonstrated in ***Figure 4-20*** and ***Figure 4-21***. As it is spotted single cross-threaded pier gives fairer scour reduction compared to double cross-threaded piers. At the upstream and downstream region for single cross-threaded pier using thread angle of 15^{o} and b/D = 0.067 has the highest value of efficiency which is 57% and 100% respectively. The double cross-threaded pier serve as a better flow damper when using thread angle of 30^{o} and b/D = 0.067 at the upstream which is 64%. By using thread angle of 30^{o} and b/D = 0.1 there is improvement in efficiency at the downstream which is 39% for double cross-threaded pier. Generally, the single cross-thread piers offer higher efficiency in reducing scour problem at its downstream.

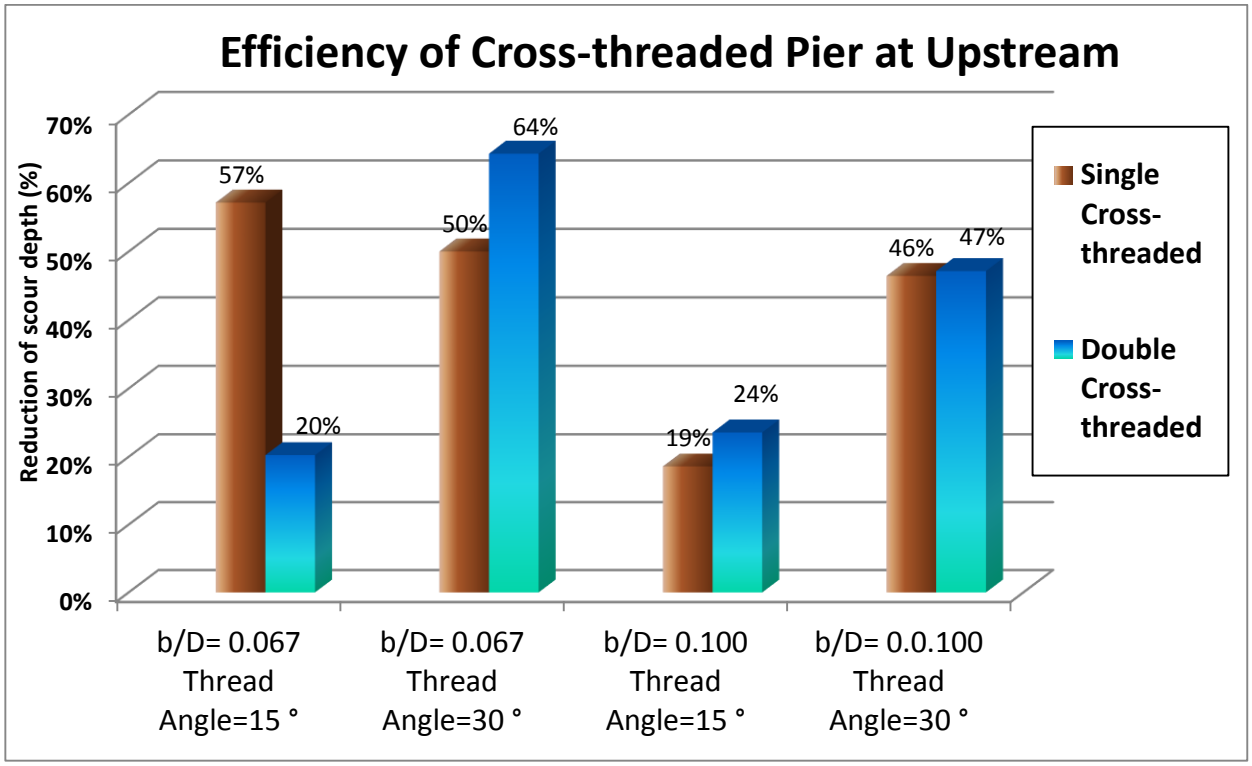

Figure 4-20*: Scour Reduction of Single and Double Cross-Threaded Pier At Upstream.*

The performance of double cross-thread pier becomes less compare to single cross-thread pier when the large cable size and small thread angle are used. This can be explained by the arrangement of the thread become too dense and it have tendency to act as a bigger pier. Increasing the number of threads will increase the overall flow roughness. This can be described by the fact that the strength of downward flow of the double crossed thread is increases and create flow confusion by large number of cable that obstructs it. In conclusion, scour problem at pier can be reduced by the use piers of single cross-threaded of smaller width and of smaller thread angle.

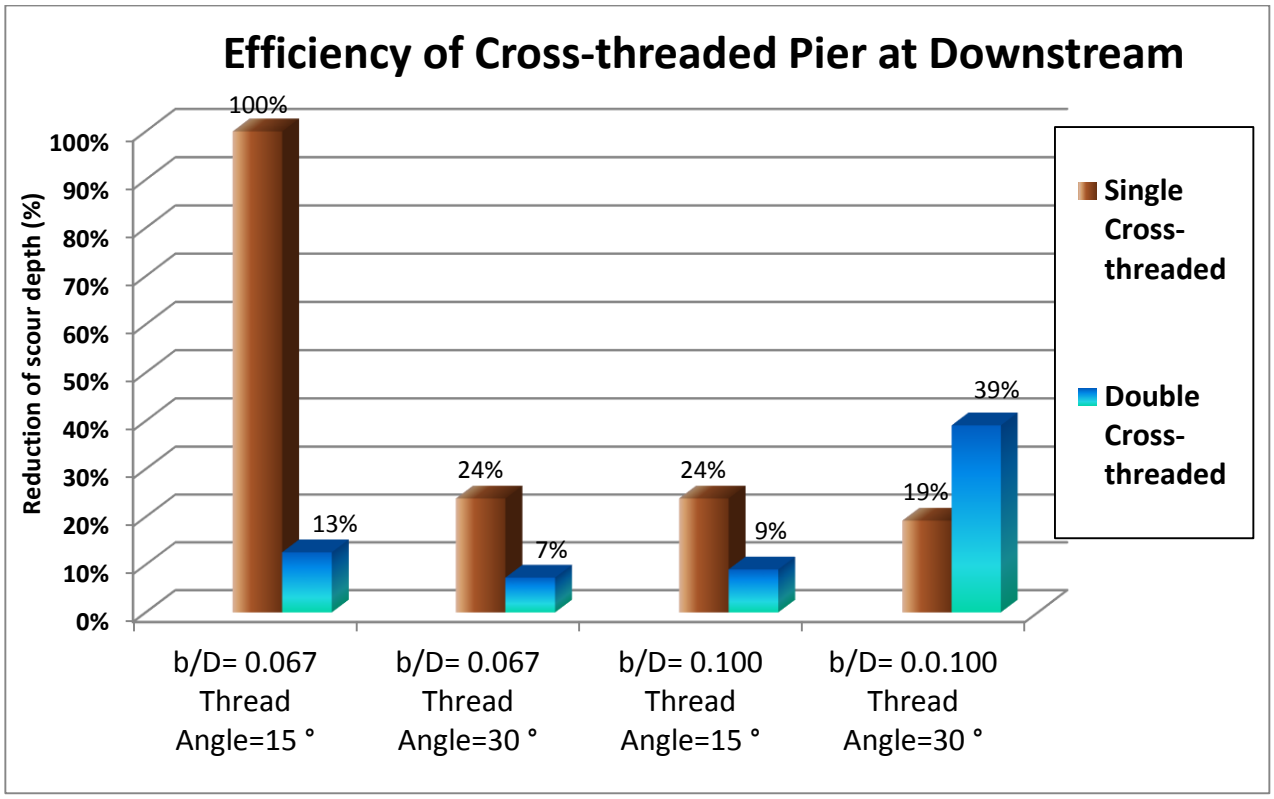

Figure 4-21: *Scour Reduction Of Single And Double Cross-Threaded Pier At Downstream.*

CHAPTER 5
CONCLUSIONS AND RECOMMENDATIONS

From the literature review, the scour depth was depended on the strength of the flow, pier size and sediment condition all the time. Large surface area of obstructing the flow also induces large vortices in forming scour. The strength of sediment in resist the erosion also affects the scour depth. The scour depth will keep increase over time until it reach equilibrium depth where the strength of vortices is equal to the resistance of sediment to erosion.

By considering the deposition and erosion pattern at the lee of pier, the cross-threaded models are able to alter the flow direction around the pier. The scour pattern for single cross-threaded are influenced by thread angle. The variation of thread angle changes the magnitude of deposition and erosion pattern of respective cable diameter. The patterns for thread angle 15° are different from thread angle 30°.Vice versa for double cross-threaded models, the scour pattern much influence by cable diameter. The pattern for cable-pier diameter ratio (b/D) of 0.067 is different from b/D of 0.1. By increasing the cable diameter, the transportation of sedimentation at lee of pier also increase with particular thread angle.

The models that were tested in this experiment able to reduce scour at the upstream of pier by weaken the strength of flow-down from scouring the sediment. The models also enhance the more efficiency of reducing scour depth at the lee of pier as the strength of wake vortices is reduced.

For overall performance of tested models for single cross-thread piers were able to reduce scour about 42% and double cross-thread pier with 28%. However, correct matching of cable diameter and thread angle will optimize the performance of the models. The test model of 15^{o} and b/D = 0.067 gave the best efficiency in reducing scour depth.

As the time constrain, only a few countermeasure able to test in this experiment. The performance of this countermeasure in preventing scour was analysed. For future study, the pier with collar protection with combination of cross-thread pier and more combination of countermeasure is recommended for better comparison of performance study. Specifically for this study, triple thread pier of Dey et al. (2006) also need conduct back as feature comparison of the single and double cross-threaded pier

For the accuracy and precision of the result, some improvements in measured instrument are suggested. Eco-sounder or bed profiler is recommended for future experiment. These instruments able to give more accurate and faster digital bed profile compare to point gauge. This also could help to generate 2D version of scouring pattern which helps to generate better discussion on the results obtained. The usage of point gauge may lead to parallax error where the eye not perpendicular to the measurement scale and the point gauge not placed correctly on the bed surface as it penetrate into the sediment. Besides, the usage of point gauge is time consuming. By using eco-sounder of bed profiler, the bed profile also be observed by vary of time without stopping the flow and saving much time. Furthermore the flume that been used is having outflow hole which is quite inaccurate even after the hole been closed by not allowing any flow out from the flume. There might be a minimal outflow of water and may reduce the accuracy of results. It is recommended that a better system of flume is been used for further studies.

REFERENCES

Beg, M., & Beg, S. (2013). Scour Reduction around Bridge Piers: *A Review. International Journal of Engineering Inventions*, 2(7), 7-15.

Chiew, Y. M., & Melville, B. M. (1987). Local scour around bridge piers. *Journal of Hydraulic Research*, 15-26.

Dey, S., Sumer, B. M., & Fredsoe, J. (2006). Control of Scour at Vertical Circular Piles under Waves and Current. *Journal of Hydraulic Engineering*, 270-279.

Dey, S., Helkjær, A., Mutlu Sumer, B., & Fredsøe, J. (2011). Scour at Vertical Piles in Sand-Clay Mixtures under Waves. *Journal of Waterway, Port, Coastal,* 1 *and Ocean Engineering*, 137(6), 324-33

Hamill, L. (1998). *Bridge hydraulics*. CRC Press.

Hoffmans, G., & Verheij, H. (1997). *Scour Manual.* Rotterdam: A.A. Balkema.

Izdiana, E., & Heidarpour, M. (2012). Simultaneous use of cable and collar to prevent local scouring around bridge pier. *International Journal of Sediment Research*, 394-401.

Mostafa, Y. E. (2012). *Design Considerations for Pile Groups Supporting Marine Structures with Respect to Scour. Engineering*, 4, 833.

Myrhaug, D., & Rue, H. (2003). Scour below pipelines and around vertical piles in random waves. *Coastal engineering*, *48*(4), 227-242.

Ong, M. C., Myrhaug, D., & Hesten, P. (2013). Scour around vertical piles due to long-crested and short-crested nonlinear random waves plus a current. *Coastal Engineering*, 73, 106-114.

Sumer, B. M., Fredsøe, J., & Christiansen, N. (1992). Scour around vertical pile in waves. *Journal of waterway, port, coastal, and ocean engineering*, 118(1), 15-31.

Sumer, B. M., & Fredsøe, J. (2001). Scour around pile in combined waves and current. J*ournal of Hydraulic Engineering*, 127(5), 403-411.

Sumer, B. M., Hatipoglu, F., & Fredsøe, J. (2007). Wave scour around a pile in sand, medium dense, and dense silt. *Journal of waterway, port, coastal, and ocean engineering, 133(1), 14-27.*

Tararojnoruz, A., Gaudio, R., & Dey, S. (2010). Flow-altering countermeasures againts scour at bridge piers: A review. *Journal of Hydraulic Research*, 411-452.

Walsh, V. M. (2013). *The Challenge of Wave Scouring Design for the Confederation Bridge*. Proto-Type, 1.

APPENDIX

Scour Pattern: Series A (Unprotected Pier)

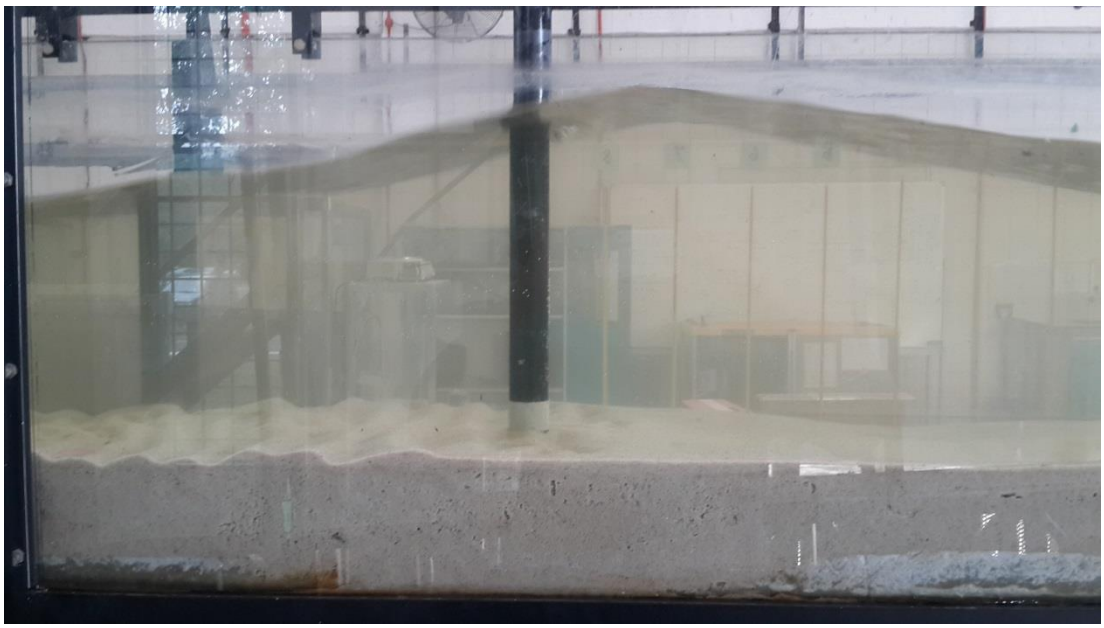

Scour Formation during Experiment

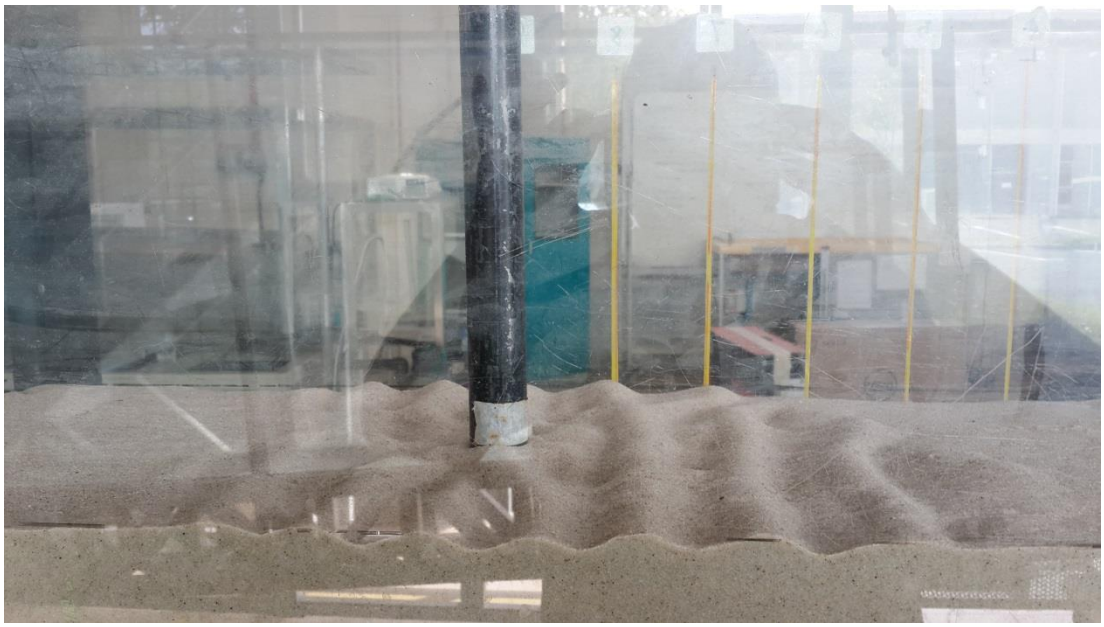

Scour Hole after Experiment

Scour Pattern: Series B (Single Cross-thread)

Scour Pattern: B1 (b/D = 0.067, θ = 15º)

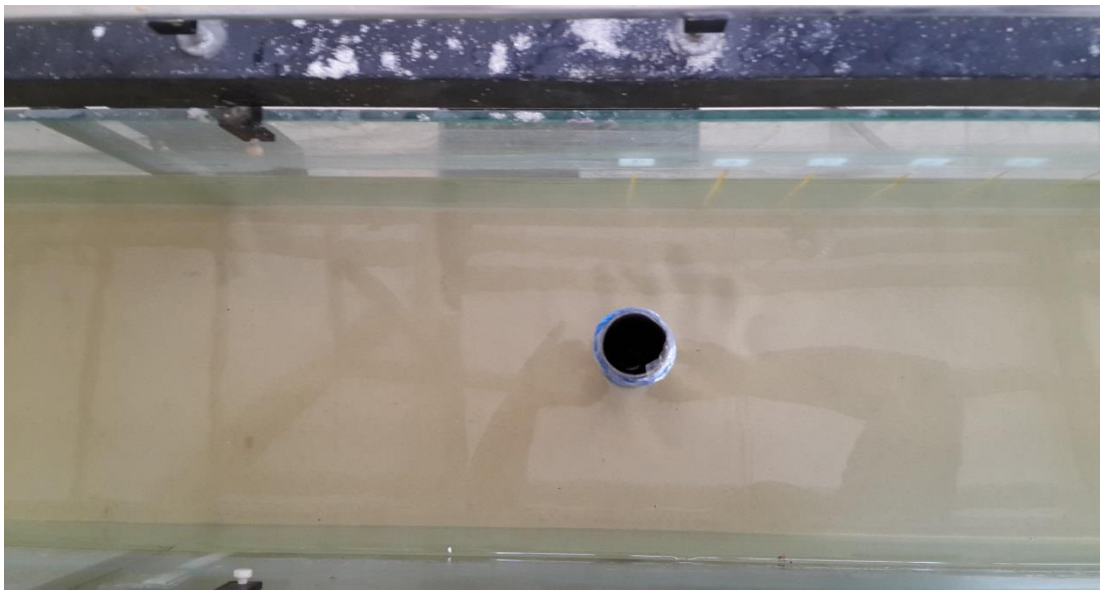

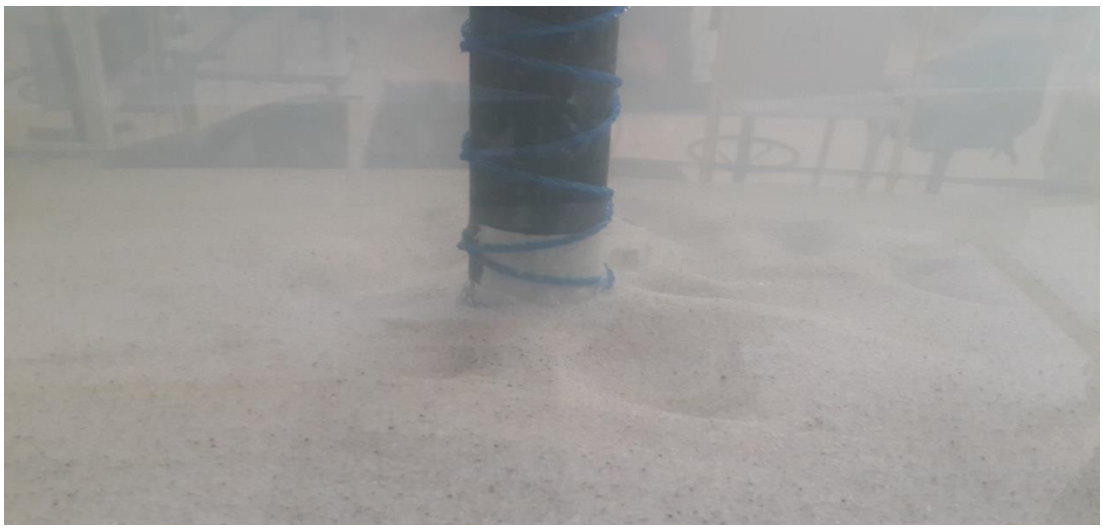

Scour Pattern: B2 (b/d = 0.067, θ = 30º)

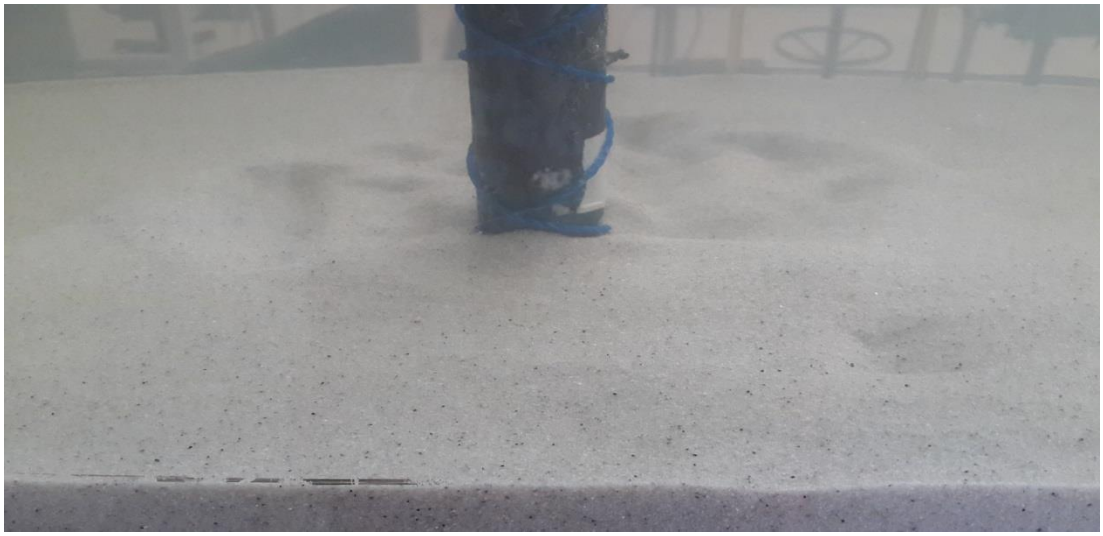

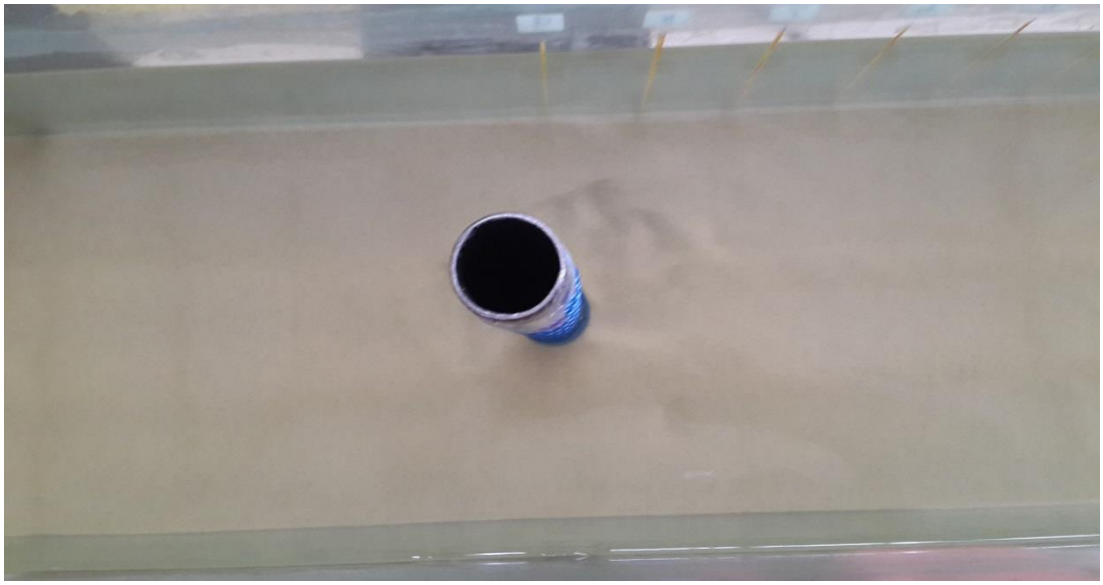

Scour Pattern: B3 (b/d = 0.1, θ = 15º)

Scour Pattern: B4 (b/d = 0.1, θ = 30º)

Scour Pattern: Series C (Double Cross-thread)

Scour Pattern: C1 (b/D = 0.067, θ = 15º)

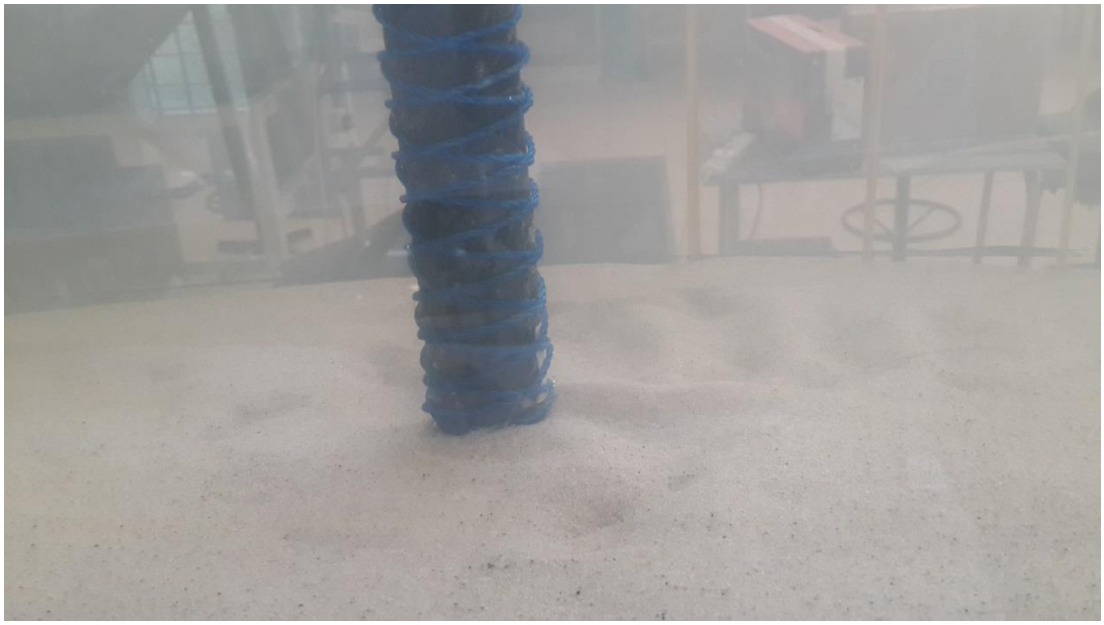

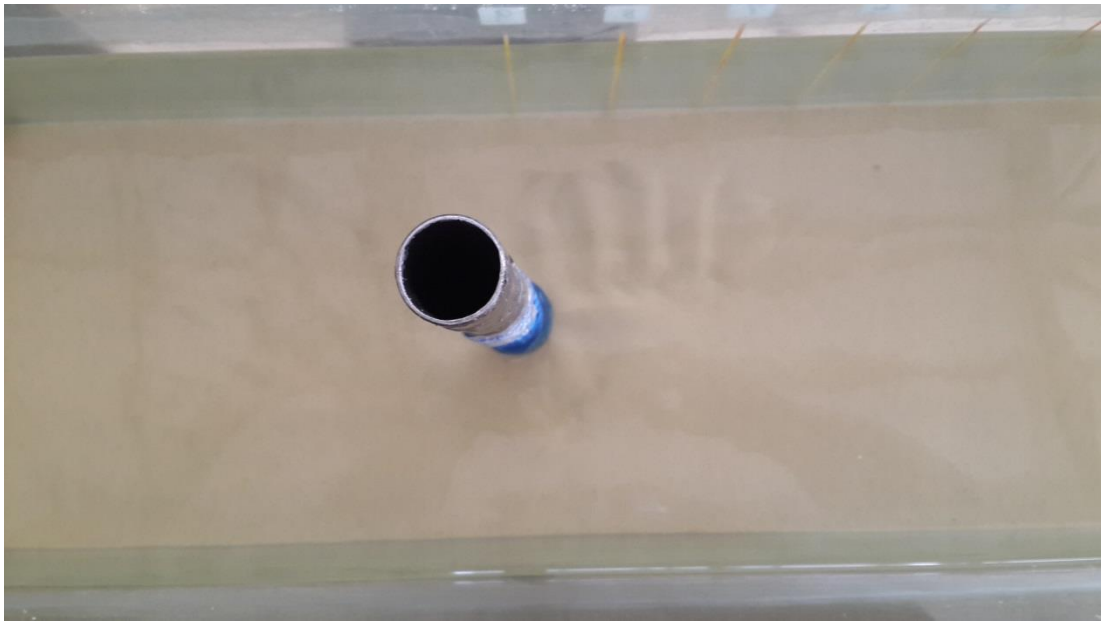

Scour Pattern: C2 (b/d = 0.067, θ = 30º)

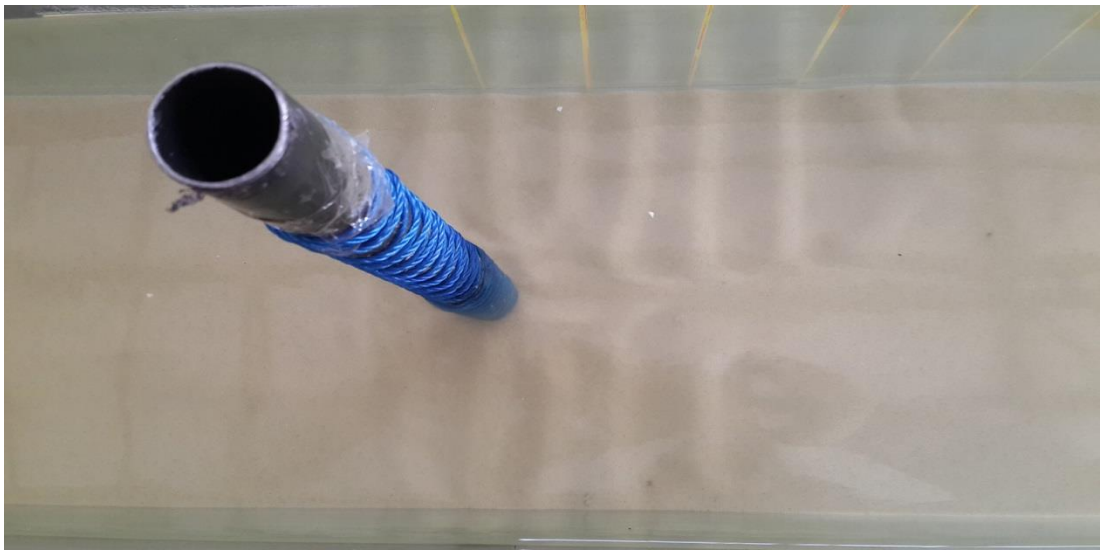

Scour Pattern: C3 (b/d = 0.1, θ = 15º)

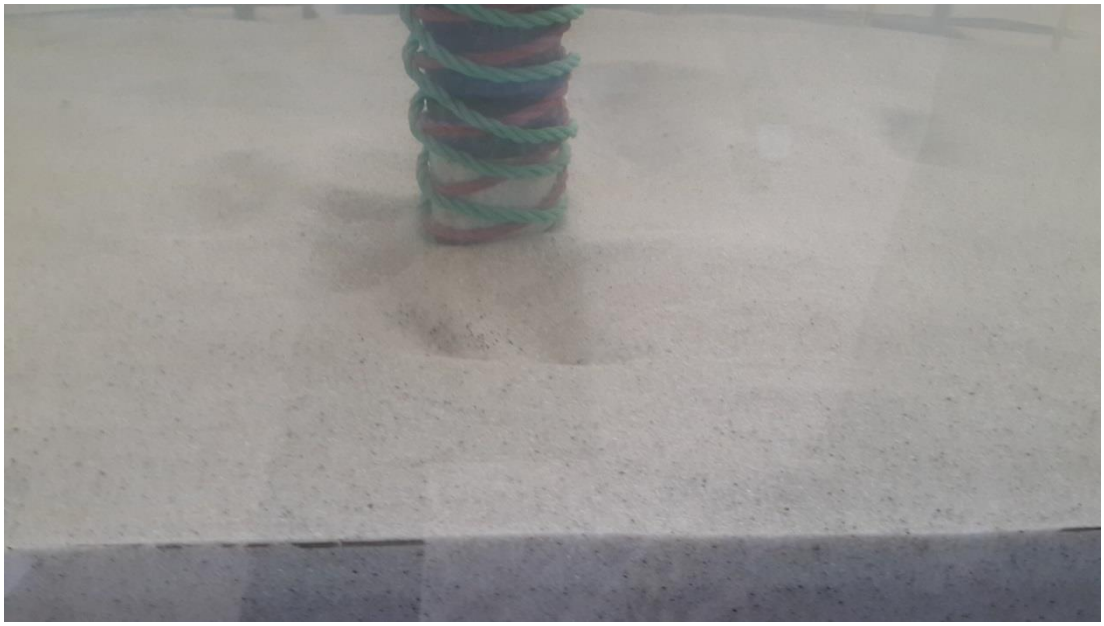

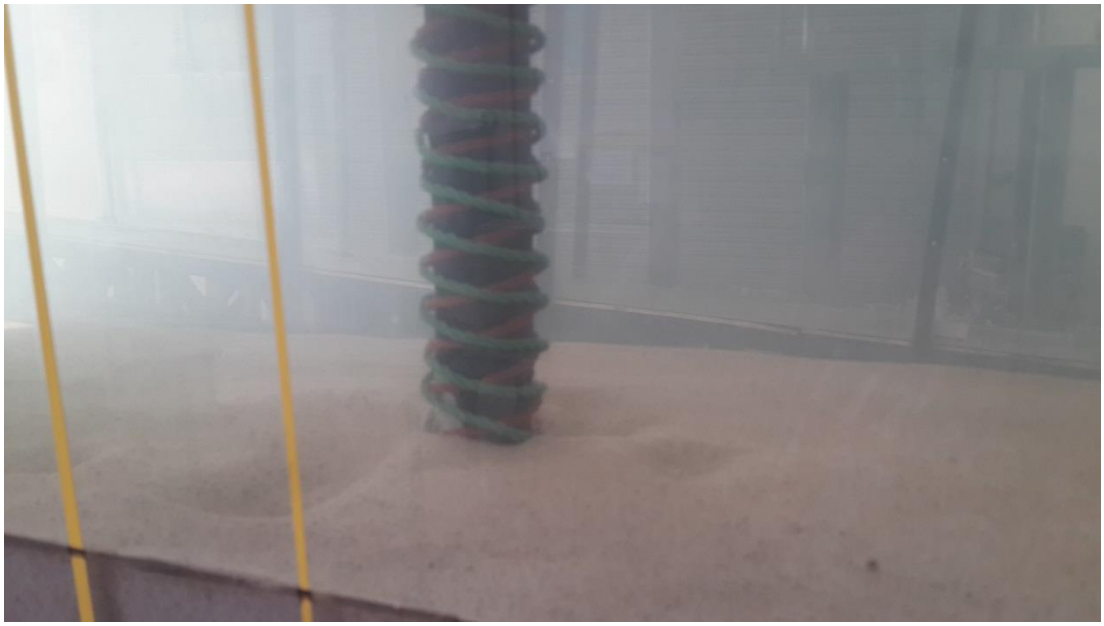

Scour Pattern: C4 (b/d = 0.1, θ = 30º)